Title: Seasonal and comparative evidence of adaptive gene expression in mammalian brain size plasticity

Authors: William R. Thomas[1], Troy Richter[2], Erin T. O'Neil[2], Cecilia Baldoni[3,4], Angelique P. Corthals[5], Dominik von Elverfeldt[6], John Nieland[7], Dina K. N. Dechmann[3,4], Richard G. Hunter[2], Liliana M. Dávalos[1,8]

[1]Department of Ecology and Evolution, Stony Brook University, Stony Brook, New York, United States
[2]Department of Psychology, Developmental and Brain Sciences Program, University of Massachusetts Boston, Boston, Massachusetts, United States
[3]Max-Planck Institute for Animal Behavior, Radolfzell, Germany
[4]University of Konstanz, Konstanz, Germany
[5]John Jay College of Criminal Justice, New York, New York, United States
[6]Department of Radiology, University Medical Center Freiburg, Freiburg, Germany
[7]Health Science and Technology, Aalborg University, Aalborg, Denmark
[8]Consortium for Inter-Disciplinary Environmental Research, Stony Brook University, Stony Brook, New York, United States
*Correspondence: *William R. Thomas (william.thomas@stonybrook.edu)*

Abstract:
Contrasting almost all other mammalian wintering strategies, Eurasian common shrews, *Sorex araneus*, endure winter by shrinking their brain, skull, and most organs, only to then regrow to breeding size the following spring. How such tiny mammals achieve this unique brain size plasticity while maintaining activity through the winter remains unknown. To discover potential adaptations underlying this trait, we analyzed seasonal differential expression in the shrew hypothalamus, a brain region that both regulates metabolic homeostasis and drastically changes size, and compared hypothalamus expression across species. We discovered seasonal variation in suites of genes involved in energy homeostasis and apoptosis, shrew-specific upregulation of genes involved in the development of the hypothalamic blood brain barrier and calcium signaling, as well as overlapping seasonal and comparative gene expression divergence in genes implicated in the development and progression of human neurological and metabolic disorders, including *CCDC22*. With high metabolic rates and facing harsh winter conditions, *Sorex araneus* have evolved both adaptive and plastic mechanisms to sense and regulate their energy budget. Many of these expression changes mirrored those identified in human neurological and metabolic disease, highlighting the interactions between metabolic homeostasis, brain size plasticity, and longevity.

Main Text

Introduction:

Typical mammalian brain development consists of unidirectional postnatal growth until reaching an adulthood maximum (*1*, *2*), but the Eurasian common shrew, *Sorex araneus*, seasonally changes the size of its body, most organs, skull, and —especially— its brain (*3–6*). In the most acute case of Dehnel's phenomenon, or seasonal size plasticity, the common shrew first grows to an initial summer maximum as a juvenile, then shrinks in autumn losing up to 18% body mass, ~20% skull volume, and 26% brain mass, reaching its winter size minimum (*3–6*). Then, in the spring prior to mating, these shrews partially or fully regrow these organs, reaching a second maximum. Dehnel's phenomenon is hypothesized to be an adaptation to decrease energy demand without slowing metabolism through plasticity, improving shrew fitness during the low temperatures and limited food supply of winter (*3*, *4*, *6–12*). Corroborating this adaptive plasticity hypothesis, Dehnel's phenomenon anticipates winter conditions and is both geographically variable (*4*) and modulated by environmental temperature (*3*). Although we have begun to reveal the molecular mechanisms of Dehnel's phenomenon (*12*), the comparative context of proposed adaptations, and commonality of processes across brain regions remain unknown. Elucidating both the genetic basis and evolutionary mechanisms underlying Dehnel's phenomenon will illuminate the molecular adaptations involved in this unusual case of mammalian brain plasticity.

As a hypothesized wintering strategy, energy metabolism is key to the evolution of Dehnel's phenomenon in *S. araneus* (*11*). Tiny mammals have limited options to survive winter conditions (*13*), and Dehnel's phenomenon is exceedingly rare as a wintering strategy. While many mammals seasonally migrate away from low-temperature, low-productivity environments, some endure these conditions by reducing their energy requirements through hibernation; a phenotype that has independently evolved many times (*14–16*). The evolution and regulation of hibernation relies upon a suite of metabolic genes (*17*, *18*), including those associated with thermogenesis, circadian rhythms, and feeding behavior. Compared to most species, *S. araneus* has astronomically large energy demands, with one the highest basal metabolic rates per unit of body mass identified in any mammal (*19*, *20*). To meet these energy requirements, *Sorex araneus* forage and feed constantly. Together with brief lifespans (~1 year) that nonetheless require surviving a single winter (*21*, *22*), these extreme metabolic demands constrain survival options for *S. araneus*. Thus, by decreasing resources devoted to energetically expensive tissue such as the brain (*23*), Dehnel's phenomenon bypasses these constraints and expands the niche of a typical small mammal during winter while allowing this fast-living, predatory shrew to remain active year round.

We hypothesize Dehnel's phenomenon, which involves metabolic shifts and inter-organ communication (*12*), has evolved through the combination of both physiological plasticity and genetic adaptation. This idea is twofold; phenotypic plasticity is not only adaptive in itself as the evolved spectrum of a trait, but can also allow populations to persist in varying environments, leading to ancillary evolutionary adaptation when given enough time and strength of selection (*24*). Thus, while temporal analysis of shrew expression can elucidate putatively adaptive plastic regulation, it will miss adaptive canalization of gene expression that has contributed to the evolution of Dehnel's phenomenon. Therefore, plastic regulatory mechanisms and proposed adaptations can be further tested via cross-species comparisons of expression divergence. These cross-species comparisons treat expression as a trait and have been used to characterize diverse vertebrate adaptations including thermal tolerance and vision loss in fish (*25–27*), the effects of whole genome duplication on expression (*28–32*), sex specific alternative splicing in birds (*33*), and patterns of expression evolution in mammalian organs (*34–37*). By incorporating these comparative approaches with seasonally varying gene expression, we can further elucidate the role of plasticity and adaption in both the regulation and evolution of Dehnel's phenomenon.

The hypothalamus is an intriguing candidate brain region for comparative analysis, as it is both the brain region with the greatest seasonal size change in shrews, and the center of bodily homeostatic maintenance across mammals. In shrews, the hypothalamus undergoes a 31.6% volume reduction in autumn through

winter, followed by a 47.8% increase in spring (*38*). Across all mammals, the hypothalamus plays a pivotal role in the maintenance of energy budgets, with functions influencing: 1) energy intake and feeding behavior, 2) energy expenditure and metabolic rate, and 3) energy deficits and storage. While such functions are important for all mammals, these are critical while wintering to maintain stable internal body temperatures as external temperatures decrease. For example, the hypothalamus can activate the sympathetic nervous system as temperatures decrease, stimulating winter thermogenesis. Thus, shrews may deploy typical mammalian hypothalamic plasticity concurrent with seasonal size plasticity. Alternatively, and considering how rare Dehnel's phenomenon is, shrews may have evolved divergent approaches, akin to naked mole rat traits, a species that lives under consistent hypoxic conditions resulting in adaptations associated with decreased oxygen and blood flow across the brain (*39*). Comparative approaches, then, may identify novel adaptations that contribute to the evolution of Dehnel's phenomenon in the shrew hypothalamus.

As the brain region able to quickly respond to change, the hypothalamus has remarkable plastic capabilities associated with metabolism (*40*), especially as environmental conditions vary between seasons and can be unpredictable. While the central nervous system (CNS) acts somewhat independently of bodily metabolism through the protective effects of the blood brain barrier (BBB), the CNS is still sensitive to bodily metabolic change. We hypothesize hypothalamic plasticity is central to the evolution and regulation of size plasticity through both environmental sensing mechanisms and signaling responses to these stimuli. Specifically, we hypothesize adaptations in the shrew: 1) hypothalamic BBB associated with dynamic metabolic fluctuations, 2) sensing of metabolic state and seasonal size through hormonal signals, mediated by BBB-crossing of insulin, ghrelin, and leptin, and 3) responses to metabolic fluctuations involving ion-dependent signaling. With limited energy inertia, shrews must continuously sense their peripheral metabolism, and a combination of receptors and selective BBB permeability in the hypothalamus allows certain molecules to relay information from the peripherals to the brain. Among the best characterized of these are the peripheral hormones insulin, ghrelin, and leptin, the latter known to excite anorexigenic and inhibit orexigenic neurons in the arcuate nucleus of the hypothalamus. Finally, according to Ramon y Cajal's neuronal doctrine (*41*), differences in brain functional responses may stem from altered synaptic firing. Thus, inter- and intracellular ion concentrations play a large role in the communication between neuronal networks by propagating signals in response to perceived environmental stimuli.

To test these hypotheses, we analyzed both the seasonal and phylogenetic variation in shrew hypothalamic expression to detect signals of adaptive plasticity. First, we aimed to identify differential expression of genes across five seasons of Dehnel's phenomenon that might promote regulatory responses to seasonal variation and can be functionally validated with cell line perturbations. Second, this analysis was paired with a comparative transcriptomics approach using hypothalamic expression data from 15 additional mammal species. These analyses infer putative adaptation by testing for branch-specific expression shifts using Ornstein-Uhlenbeck models. The objective of these evolutionary analyses was to quantify lineage-specific hypothalamic expression changes in *S. araneus*, with evolutionary expression divergence consistent with selection. Finally, by comparing individual genes and associated pathways from these two analyses, we can determine potential adaptive plasticity, indicating mechanisms that both potentially regulate size plasticity and were selected for higher expression in the evolution of Dehnel's phenomenon . Our expression results implicate several key processes in Dehnel's phenomenon, including seasonal plasticity in feeding behavior, enhanced modulation of both hypothalamic blood brain barrier and downstream signaling, and plastic apoptosis responses.

Results

Temporal Expression

We identified several known neural signaling pathways correlated with patterns of seasonal hypothalamus expression that may be associated with changes during Dehnel's phenomenon. We began by hierarchically clustering expression to identify patterns of gene expression through time. Most genes did not exhibit much variation through time, indicating constitutive gene expression in the hypothalamus, as only 786 of 19,296 genes passed our filters (>0.5-fold change between any two seasons and 2 samples > 10 normalized reads). We identified 12 distinct clusters of gene expression patterns by bootstrapping (n=20) a gap statistic within cluster distances. Of these 12 clusters, five clusters consisting of 392 genes resembled a large divergence between summer juveniles and the remaining individuals without a second local maximum during size change (Supplemental Figure 2; Clusters 2, 3, 8, 11, 12). These genes likely represent a large developmental shift between recently postnatal shrews and the remainder of individuals compared to shifts associated with seasonality or Dehnel's phenomenon. We then functionally characterized the remaining 394 genes (Figure 1A), which exhibited seasonal shifts, with a GO pathway enrichment using the Database for Annotation, Visualization, and Integrated Discovery (DAVID) Gene Functional Classification Tool. Although no enrichment pathway was significant after a Bonferroni correction, 14 pathways were enriched prior to correction ($p < 0.05$; Modified Fisher's Exact Test); with the five pathways with the lowest p-values including fluid shear stress and atherosclerosis, relaxin signaling, neuroactive ligand-receptor interaction, HIF-1 signaling, and PI3K-Akt signaling (Figure 1B). Many of these pathways have been implicated in various physiological processes, which suggests that variation identified in the hypothalamus are likely the result of autonomic processes in homeostatic maintenance. Individual enrichments of each pathway can be found in Supplemental Table 2.

We also discovered hundreds of differentially expressed genes between autumn and spring shrews that may mediate phenotypic divergence in both size (shrinkage vs. regrowth) and metabolic changes (liver expression shifts (*12*)) associated with Dehnel's phenomenon. By comparing the RNA expression of autumn and spring shrews, we found 210 differentially expressed genes (DEGs), with 129 upregulated and 81 downregulated in spring (Figure 2A). We ran a GO pathway enrichment to functionally characterize the 210 DEGs in the hypothalamus and found fifteen pathways were enriched ($p<0.05$; Modified Fisher's Exact Test) with significant genes prior to multiple comparison correction. These pathways were all downregulated in spring and included; pathways in cancer (4.5-fold enrichment, $p<0.001$), transcriptional misregulation in cancer (8.3-fold enrichment, $p<0.001$), fluid shear stress and atherosclerosis (9.5-fold enrichment, $p<0.01$), small cell lung cancer (11.5-fold enrichment, $p<0.01$), IL-17 signaling (11.3-fold enrichment, $p<0.01$), cAMP signaling (5.9-fold enrichment, $p<0.01$), and apoptosis (7.8-fold enrichment, $p<0.05$) (Figure 2B). Pathways in cancer consisted of nine significantly downregulated genes (from DESeq2 Wald test), four of which overlapped with apoptotic pathways including *BCL2L1* (-0.6 Log-Fold Change [LFC] $p_{adj}<0.01$), *NFKBIA* (-1.3 LFC, $p_{adj}<0.01$), *FOS* (-1.5 LFC, $p_{adj}<0.05$), and *GADD45B* (-1.4 LFC, $p_{adj}<0.05$) (Figure 2C). Differential expression for all genes can be found in Supplemental Data. Overall, the processes identified suggest regulation of cell proliferation (cancer pathways) and death (apoptosis) in the hypothalamus may be associated with phenotypic changes during Dehnel's phenomenon .

Cell Viability Analysis with BCL2L1 Overexpression

We examined the potential functional effects of apoptosis regulating gene, *BCL2L1* (Figure 2D), which was differentially expressed between seasons, by propagating an *in vitro* model of domesticated ferret brain cells (MPF-CRL-1656, ATCC). We chose this cell line because there is no established cell line of *Sorex araneus*. *Mustela putorius furo* also undergoes a Dehnel's-like phenotype (*42*) and is more closely related to shrews than mice are. MPF cells were transfected with either the anti-apoptotic *BCL2L1* RNA or a scrambled version of *BCL2L1* (sBCL2L1) RNA. 24 hours after transfection, cells were exposed to heat stress followed by crystal violet staining. A significant difference in cell viability was observed between the heat scrambled compared to the control scrambled groups (df=3.56, $t_{3.56}=8.78$, $p<0.01$),

however, there was no significant difference between cells transfected with *BCL2L1* compared to those transfected with sBCL2L1 when exposed to heat (df=3.37, $t_{3.37}$=-0.99, p=0.39).

Evolutionary Divergence in Expression

Analyses quantifying branch-specific shifts in expression identified hundreds of genes that were upregulated in the shrew hypothalamus (post pubescent spring individuals) compared to other mammals, suggesting adaptation for increased expression in these genes (Figure 3). EVE models found 222 genes significantly rejected ($p_{adj} < 0.05$) a single expression optimum for all species in favor of a second expression optimum for the shrew lineage. Notably, all second optima (in the shrew lineage) were higher than the first optimum, consistent with results from the original methods manuscript (*34*). While nonsignificant genes had a mean 0.93-fold change, genes experiencing an expression branch-shift in shrews had a mean 9.66 oTPM-fold change compared to other species. To validate genes with expression branch-shifts as shrew-specific, we ran a dropout test for the shrew lineage, testing for phylogeny-wide evidence of selection for each gene. Of the 6,496 genes tested, 81 genes had significantly ($p_{adj} < 0.05$) lower β (within population variance to between species variance), suggesting selection elsewhere in the phylogeny. None of these genes overlapped with those identified to be differentially expressed in the shrew, further validating the specificity of expression shifts.

We identified several changes associated with processes that may underlie seasonal size plasticity. Pathway enrichment analysis identified two significantly enriched pathways: calcium signaling (2.8-fold enrichment, p<0.05) and autophagy (9.1-fold enrichment, p<0.05) (Figure 3). Upon manual inspection of the list, we also identified several other potential adaptive processes, including blood-brain-barrier formation and function, feeding behavior and leptin responses, metabolism, and neuroprotection. (Figure 3, Table 1).

Many of these putative adaptations mediate responses to environmental cues centered around energy demands. Four of the genes experiencing branch-shift changes in expression were also differentially expressed between autumn and spring individuals, suggesting not only an adaptive shift in the shrew lineage associated with the evolution of Dehnel's phenomenon, but also a direct molecular mechanism for brain changes. The four genes that overlap between both analyses include (Figure 4): *CCDC22*, which plays an important role in endosomal recycling of membrane proteins (*43*); *LMX1A*, a transcription factor essential for dopaminergic neuron development (*44*); KCNS1, which encodes a subunit of potassium channels associated with neuronal excitability and pain sensitivity (*45*); and *PAQR4*, which appears to regulate growth and apoptosis through sphingolipid synthesis in human cancers (*46*). However, identifying four overlapping genes is not significantly greater than expected by chance (Fisher's Exact Test, p=0.55)

Discussion

By characterizing both seasonal and between-species differential expression of the hypothalamus, we generated and probed a unique data set, discovering expression shifts associated with extreme brain and body size plasticity in *Sorex araneus*. While the focus on seasonal hypothalamus expression provided insights into both the regulation of seasonal homeostasis and processes underlying brain size change, evolutionary shifts in expression revealed putative adaptations associated with mammalian brain degeneration and regeneration in a natural system. Our analyses identified a suite of genes related to energy homeostasis and environmental sensing that were either seasonally plastic or upregulated in the shrew compared to other mammals, reinforcing the profound role of metabolism in the evolution and regulation of Dehnel's phenomenon. We also found seasonal changes in genes associated with cancer pathways and apoptosis, indicating that the regulation of cell proliferation and death is critical during brain size change. Notably, some of these results resemble expression changes found in human neurological and metabolic disease, which may prove important for future research on therapeutic treatments.

Seasonal plasticity associated with maintaining metabolic homeostasis

Dehnel's phenomenon has been proposed to permit winter activity by reducing shrew energy requirements by limiting energy devoted to the maintenance of larger tissues (*4*, *7*, *20*). This suggests that the maintenance of homeostasis, especially processes related to energy balance, is critical during Dehnel's phenomenon. Seasonal hypothalamus expression data corroborate this hypothesis, as we found three pathways enriched with seasonally varying genes in the hypothalamus with metabolic associations: relaxin signaling, phosphoinositide-3 kinase (PI3K) signaling, and neuron ligand receptor interactions. Relaxin, a neuropeptide, plays a pivotal role in many physiological functions in model organisms, including food and water intake (*47–50*); food restriction upregulates relaxin-3 (*RLN3*) *in vivo* (*51*), while administering RLN3 protein into the rat hypothalamus vastly increases food intake (*52–55*). Relaxin has also been found to activate the PI3K pathway (*56*, *57*), which mediates feeding behavior and glucose homeostasis (*58–62*), as well as angiogenesis via vascular endothelial growth factor (VEGF) production (*57*, *63*, *64*). PI3Ks activity influences feeding behavior and weight gain in response to key metabolic hormones, including leptin and insulin (*60–62*, *65*). Lastly, the neuroactive ligand-receptor interaction pathway, a subclass of Kyoto Encyclopedia of Genes and Genomes (KEGG) Environmental Information Processing pathway, is associated with responses in model organisms to shifts in diet (*66*), stress (*67*), and temperature (*68*, *69*), all of which the shrew experiences during seasonal changes. Although exploration of gene function in *S. araneus* has only begun, seasonal expression in the hypothalamus highlights that while remaining active in winter with high metabolic rates (*20*), shrews actively regulate feeding behavior, food intake, and energy homeostasis.

Putative hypothalamus adaptations may enhance regulatory responses

Sorex araneus have disproportionately high metabolic rates (*20*), which they must maintain in winter. While seasonal transcriptomics indicate active regulation of processes related to energy homeostasis, we hypothesized that natural selection may select for effective strategies in comparison to other mammals. To test this, we used comparative analyses which indicated shrews may have evolved adaptive environmental sensing. We found upregulation of several proangiogenic genes associated with the formation and function of the blood brain barrier, including *VEGFA* and *WNT7A*. In normal neural development, neural progenitor cells and surrounding astro- and pericytes express these two genes defining an expression gradient that guides blood vessels to form the blood brain barrier (*70–72*).

While this suggests *VEGFA* and *WNT7A* upregulation in the shrew may increase vascularization of the brain, continued expression of *VEGFA* beyond development increases BBB permeability, leading to a breakdown of its protective effects (*73*, *74*). BBB permeability is a common symptom of many disease-like states including neuroinflammation (*75*) and neurodegeneration (*75–77*). The hypothalamus BBB consists of tanycytes and highly fenestrated capillaries with less tight junctions (*78*), replacing the less permeable BBB of other brain regions with a specialized barrier that improves nutrient and energy sensing through dynamic passage of molecules from peripheral circulation (*79–81*). Experiments on mice indicate reduced blood glucose levels from fasting promote capillary fenestration in the hypothalamic BBB via upregulation of *VEGFA*, eliciting feeding responses through increased hypothalamic exposure to glucose levels (*79*). In shrews, upregulation of *VEGFA* and *WNT7A* may constitutively increase capillary fenestration, a potential adaptation of the BBB to improve hypothalamus metabolic sensing and signaling in response to high energy demands. Notably, adaptive expression of *VEGFA* has also been identified in the seasonal vascular plasticity of other mammal species, including reproductive sheep (*82*, *83*), bison (*84*), and squirrels (*85*), thus shrew upregulation of *VEGFA* to meet unusually high metabolic demands may parallel mechanisms used seasonally in reproduction.

We also found evidence for adaptive expression relating to maintenance of energy balance, specifically in feeding behavior and leptin responses. Key genes associated with the hypothalamic leptin response, such as *NPY*, *AgRP*, or *POMC*, were not universally orthologous and so could not be analyzed, but there was

evolutionary upregulation of many genes involved in downstream leptin responses (*FOXO4*, *GRB2*, *IRX5*, *AGT*) (Figure 3, Table 1). Unlike their upstream effectors, these genes may have subtle effects on continuous feeding behavior. For example, in the hypothalamus FOXO1 negatively regulates POMC and promotes AgRP expression (*86*), which can contribute to leptin resistance resulting in a long term appetite suppression (*87–89*). However, much less is known about the hypothalamic functions of the *FOXO1* paralog, *FOXO4*. In mouse adipocytes, leptin- dependent expression of *FOXO4* can rapidly clear blood glucose levels (*90*), which can lead to energy storage and decreased satiety. We hypothesize that, in shrews, upregulation of *FOXO4* could either increase blood glucose clearance or leptin resistance, reducing long term satiation and promoting continuous feeding. Functionally, evolutionary upregulation of these genes in the shrew hypothalamus may result in evolved leptin insensitivity, instead of the development of leptin resistance. Reduced leptin sensitivity in shrews could reduce overall satiation, promoting foraging even when the short-term energy budget is balanced thereby improving anticipatory storage before winter.

Lastly, calcium signaling is a ubiquitous form of neural communication (*91*, *92*) that occurs through the regulation of intra and extracellular calcium concentrations, transmitting signals that can release neurotransmitters (*93*, *94*) and promote gene expression (*95–98*). Thus, it has been implicated in numerous functions including dendrite growth (*99*, *100*), synaptogenesis (*101–103*), and initiation and maintenance of long-term potentiation (*104*, *105*). In shrews, adaptive calcium signaling through the upregulation of several calcium-responsive genes (*VEGFA*, *CASQ1*, *HRH2*, *TACR2*, *PPIF*, *SPHK2*, *GRIN1*) may improve environmental information relay in the hypothalamus, both internally and throughout the central nervous system.

Evolution of brain size plasticity: roles of cellular proliferation, death, and links to neurological disease

Progressive cell loss in neurons is a hallmark of neurodegeneration (*106*), but despite seasonal decreases in brain mass and volume, shrews show no reduction in cell number (*107*). Uncorrelated changes in size and neuron count in shrews might suggest they evolved neuroprotective mechanisms to reduce cell loss associated with decreased brain size. We found an enrichment of genes upregulated in autumn shrews involved in cancer pathways and apoptosis regulation. The processes underlying cancer and neurodegeneration oppose one another, with increased resistance to cell death driving cancer and premature cell death driving neurodegeneration. Shrews appear to traverse this tightrope by regulating these pathways to avoid both the cell loss typical of neurodegeneration and unchecked proliferation of cancer. This may represent a unique neuroprotective mechanism.

BCL2L1-mediated apoptosis seems to play a critical role in helping shrews maintain this balance during seasonal size change. As a known anti-apoptotic gene, *BCL2L1* promotes cell survival by reducing apoptosis through an NFKB-dependent pathway, as demonstrated in rodents (*108–110*). The BCL2 gene family is also recognized for its contrasting roles in disease, with upregulation in central nervous system disorders and downregulation in cancers. We found an enrichment of the apoptosis pathway with upregulated genes in autumn, including *BCL2L1*, which may explain why shrews do not exhibit the neuronal loss typically associated with human neurodegeneration. This suggests that the mechanism parallels aspects of neurodegenerative disease without the associated pathology, which we propose could be another neuroprotective mechanism to reduce cell death during brain shrinkage in shrews.

The regulation of apoptosis may represent a convergently evolved strategy across species managing environmental and metabolic stress. For example, natural experiments in hibernators found seasonal reduction of apoptosis, paired with upregulation of *BCL2L1* (*111*, *112*), including in the brain (*113*). Specific to Dehnel's phenomenon, *BCL2L1* upregulation in autumn indicates tight regulation of cell survival during brain size changes and periods of metabolic and environmental stress: a balance between brain shrinkage and maintenance of cell numbers.

Evolutionary change in shrew gene expression likely benefits this cellular regulation. We found an evolutionary upregulation of genes associated with autophagy, which is the degradation of cellular parts to provide energy and materials to maintain cellular homeostasis under stressful conditions, in the shrew hypothalamus. This included *MLST8*, an integral component of the mTOR protein complex 1 (mTORC1) that regulates sugar and lipid metabolism(*114*), but also has recently been found to modulate autophagy in response to nutrient deprivation (*115*). Two evolutionarily upregulated genes *PPIF* and *SPHK2*, can also promote apoptosis associated with mitochondrial calcium influx. PPIF is an important component of the mitochondrial permeability transition, which responds to cellular calcium overload and oxidative stress by promoting cell death (*116–119*). Similar to *PPIF*, overexpression of *SPHK2* in stressed cells induces cell cycle arrest and promotes apoptosis through a series of signaling cascades that increase cytosolic calcium and promote the release of pro-apoptotic cytochrome C from the mitochondria (*120*, *121*). While both *SPHK2* and *PPIF* are overexpressed and likely contribute to neuronal death in both human patients with Huntington's disease or Alzheimer's disease and rodent models of these diseases, knockout or inhibition of these genes protects against neurodegeneration (*122–125*). In the shrew hypothalamus, canalized upregulation of these genes likely influences cell survival and death, but precisely how requires further investigation.

Lastly, *CCDC22*, *KCNS1*, *LMX1A*, and *PAQR4*, are both seasonally plastic and evolutionarily upregulated in the shrew hypothalamus (Figure 4). While the number of overlapping genes is not significantly greater than expected by chance, the combination of seasonal and evolutionary upregulation suggests these genes may play integral roles in Dehnel's phenomenon. Notably, some of these genes are directly related to the development and progression of neurological disorders in humans. For example, CCDC22 regulation in shrews may provide protection against harm incurred during seasonal size changes. The coiled-coil domain containing 22 protein (CCDC22) plays a key role in endosomal recycling of proteins and is a novel candidate gene for several neurological disorders (*126–129*). CCDC22 is a subunit of the CCC (CCDC22, CCDC93, COMMD) complex that aids in trafficking and recycling of endosomal membrane proteins (*43*, *130*, *131*). Improper recycling and resulting protein aggregation readily occurs in neurons, as they do not proliferate (*132*, *133*), and has also been implicated in neurodegenerative diseases, including cytotoxicity in amyotrophic lateral sclerosis (*134*), amyloid-B aggregation in Alzheimer's disease (*135–137*), and MUL1 degradation in Parkinson's disease (*138*). Missense mutations and subsequent downregulation of CCDC22, are potential mechanisms underlying X-linked intellectual disability (*126*, *127*) and Ritscher-Schinzel syndrome (*127–129*) in humans. Both disorders are characterized by macrocephaly, malformations of the brain, craniofacial abnormalities, and intellectual disabilities. In pubescent spring shrews, we found CCDC22 has a ~7-fold upregulation compared to other mammals and a significant upregulation during spring compared to autumn shrinkage. Neuroprotective functions may be especially important in spring, as brain mass returns increasing the need for endosomal recycling of proteins and may explain seasonal plasticity in *CCDC22* expression in tandem with adaptive upregulation.

Limitations

Despite the proposed adaptive roles of the many genes discussed in our study, several limitations must be acknowledged. During shrew seasonal size plasticity, shrew environments may differ from those of the other species included in this experiment. These environmental differences could influence gene expression, leading to over- or underestimation of selection in the shrew lineage. Although we controlled for several sources of variation by using only pubescent and wild or non-domesticated individuals when feasible, other sources of variation remain unaccounted for because of practical constraints. The functions we propose for many genes remain speculative and require further validation. For example, we tested the hypothesis that autumn upregulation of *BCL2L1* reduces apoptosis by overexpressing this gene in a related mammalian neural cell line. However, this experiment did not demonstrate a rescue effect against heat-induced apoptosis, contrary to our expectations. While this unexpected result could stem from several causes, such as the anti-apoptotic function of *BCL2L1* being specific to the unique neural

environment of shrews or arise through species-specific gene interactions, it may also reflect limitations in our study, highlighting the need for further investigation to validate and refine our conclusions.

Conclusion

We discovered evidence for adaptive evolution of gene expression involved in the regulation of metabolism, cell survival, and size plasticity associated with Dehnel's phenomenon. Not only does the hypothalamus shrink to reduce energetic load during winter, but it must also control metabolic homeostasis during these changes. Our results reveal both conserved and novel gene expression mechanisms that likely underlie the central functions of the hypothalamus during seasonal size plasticity. While previous work had hinted at the metabolic nature of Dehnel's phenomenon, by pairing seasonal differential expression with comparisons to other species, we identified adaptations likely involved in the evolution of this unique brain size plasticity. Metabolism, body size, and longevity are intrinsically linked life history factors. In the shrew, unusually high metabolic rates force winter activity, leading to intense metabolic sensing and regulation, changes in cell survival pathways, and –through both the evolution of Dehnel's phenomenon and these sensing and regulatory adaptations– shortened lifespans. Together, these gene expression adaptations likely underlie drastic seasonal size change and mitigate its detrimental effects.

Materials and Methods

Shrew Sample Collection

We used tissues from shrews collected for experiments analyzing gene expression and metabolic shifts in brain regions through Dehnel's phenomenon (*12*). Briefly, S. *araneus* were collected from a single German population (47.9684N, 8.9761 E) across five different seasons of Dehnel's phenomenon from June 2020-June 2021 (n=25, n_{per_season} = 4-5). Shrews were trapped with insulated wooden traps that contained mealworms, which were checked every two hours. This protocol was used to minimize trap-related stress from heat/cold shock or lack of food and thus reduce stress-related variation on gene expression. Shrews were then euthanized via vascular perfusion of PAXgene Tissue Fixative. Brain regions were dissected into individual regions in cold fixative and then incubated in PAXgene Tissue Stabilizer for 2-24 hours before long-term storage. Samples were preserved in stabilizer at -180°C in liquid nitrogen until RNA extraction.

RNA Extraction, Library Preparation, and Sequencing

We extracted the *S. araneus* hypothalamus RNA using a modified Qiagen Micro RNAeasy protocol used for small mammalian sensory tissues (*139*). These extractions reduce degradation due to heat and improve RIN from standard Qiagen Micro RNAeasy protocols by disrupting tissue on dry ice using glass, instead of plastic, mortar and pestles. RNA was sent to Azenta Life Sciences for quality control (nanodrop and RNA ScreenTape), library preparation, and sequencing. Hypothalamus libraries were prepared with poly-A selection and sequenced for approximately 15-25 million reads per sample in 150bp PE reads.

RNA sequences from other species were collected from the NIH National Center for Biotechnology Information's (NCBI) Sequence Read Archive data sets. First, we searched the Sequencing Read Archives (SRA) for the keyword hypothalamus, filtered by both RNA and mammal species. As models described below rely on using the variance both between and within species, species required three or more biological samples to be included. This removed any species that had only one hypothalamus sample sequenced. Species were excluded from the study if a genome assembly was not readily available (*Phodopus sungorus*), as this information was needed for an unbiased alignment of reads. Our final criterion was to only include species for which post-pubescent individuals were available to reduce noise from age effects and the onset of puberty. If the onset of puberty was not specifically stated for the dataset, AnAge (*140*) was used to determine if samples were pubescent. *Oryctolagus cuniculus* and *Pan paniscus* were prepubescent and thus removed. For the remaining species, if multiple hypothalamus RNA-seq data sets were available, we used less stringent rules to determine which data to select. First, to

reduce domestication or captivity effects, we chose wild or non-domesticated individuals over laboratory-raised animals. Second, to reduce the variance from different extraction protocols and sequencing methods, we used samples from the same experiments or larger data sets, available for multiple species or brain regions. Using samples from datasets with multiple regions or species also suggests intimate knowledge of neural anatomy, increasing confidence in dissections. Third, we used a maximum of eight samples per species and attempted to maintain a 1:1 sex ratio when possible. We did not filter by sequencing method (e.g., used 50bp SE as well as 150 PE reads) or sequencing depth, as filtering poor reads and normalizing for library depth and content should account for both these factors.

RNA Quantification, Normalization, and Orthology

Adapter sequences were trimmed from the raw reads using the default parameters of fastp (*141*), which is able to autodetect adapters regardless of different library preparations across species. This program also corrected and pruned low quality bases and reads using a sliding window approach. Processed reads were aligned and quantified with Kallisto 0.46.2 (*142*), which probabilistically estimates gene counts through pseudo-alignment to each species-specific genome assembly. Samples were removed from the data set if mapping rate was below 30%, indicating either poor sequencing or low assembly quality. Additionally, novel shrew hypothalamus sequences were compared against previously published shrew region data to verify tissue type. Gene counts for all species were then normalized for total library size into Transcripts Per Million (TPM). Orthologous genes between species were inferred with OrthoFinder (*143*) using default parameters, retaining only single-copy orthologs identified across all species (n=6,496 single-copy orthologs). Visualizations of the frequency distribution of the orthologous (oTPMs; Supplemental Figure 1) were used to identify outlier species. For example, *Papio anubis* was removed from this experiment because of its extremely low mapping percentage (mean 16.75%; range 9.5%-23.7%), which had a large effect on the oTPM distribution.

Branch-shift Changes in Expression

We modeled gene expression as a trait using phylogenetic comparative methods, as these account for evolutionary divergence among species (*144*). We ran Expression Variance and Evolution models (EVE) to test for significant changes of expression in the shrew lineage, using post pubescent spring individuals (*34*). EVE models both parameterize and estimate the ratio (β) of population (within species) to evolutionary (between species) variance, such that high β ratios indicate expression plasticity, and low β ratios indicate differential expression between species, necessary for inferring selection. We ran two EVE models to test for divergence in expression in the shrew lineage. First, we tested for branch-specific expression level shifts by contrasting the likelihood of two Ornstein-Uhlenbeck models for the data, one with a single expression optimum (null; stabilizing selection), and another with a second optimum on the shrew branch (selection). A likelihood ratio test between the null and selective hypotheses for each gene (χ_1^2) was conducted using these likelihoods. A Bonferroni correction was used to account for multiple hypothesis tests to identify candidate genes under selection (p_{adj}<.05). For the second model, we ran a dropout test to further validate the specificity of the expression change in the shrew lineage. After removing the shrew expression data, we identified genes with high expression divergence across the phylogeny (significantly low β ratios), which would indicate relaxed or diversifying selection. This gene list was compared to that from first model to prune genes not specifically associated with divergence in the shrew. Both models described above ran on the Bayesian molecular-clock mammalian phylogeny of (*145*) pruned to match our species sample. Finally, we used the DAVID functional annotation tool (*146*) to determine enriched KEGG Gene Ontology (GO) pathways from the candidate gene set.

Temporal Clustering

To analyze the temporal variation of shrew expression in the hypothalamus, we temporally clustered our data using the package TCseq (*147*). We began by further normalizing our data across Dehnel's phenomenon seasons using the median of ratios from DESeq2 (*148*), which normalized for library size and content. Genes with consistent expression across time with little variation between seasons would not be associated with observed phenotypic changes. These genes were filtered from this data set by only selecting genes with an absolute fold change of 0.5 between any two seasons. We also removed genes with low expression that would appear to have high fold changes despite lacking enough transcript expression to influence phenotype, retaining only reads with two samples > 10 normalized reads. After filtering, counts for each season were converted to mean z-scores and then clustered into groups of similar gene expression profiles using fuzzy cmeans clustering. The number of resulting gene clusters was calculated a priori, by bootstrapping (n=20) a gap statistic that minimizes within-cluster distances. Genes with highest membership in clusters associated with variation across all seasons (seasonal effect; Clusters 1, 4, 5, 6, 7, 9, 10), as compared to those that just show extensive differences (>1.25 standard deviations) between the summer seasons (juvenile and adult) without a second local maximum (abs(autumn-winter)<0.5 and abs(winter-summer adult)<0.5) (developmental effect; Clusters 2, 3, 8, 11, 12), were analyzed for KEGG GO enrichment using DAVID functional annotation (*146*). Additionally, each cluster was analyzed individually and included in the Supplementary Material.

Differential Gene Expression

We tested for differential gene expression between autumn and spring individuals, as these seasons differ in hypothalamic size phenotype (shrinkage vs. regrowth) (*38*), and were previously identified divergence in liver expression related to metabolism (*12*). To test for significant differential expression, we fit a negative binomial generalized linear model to the normalized (median of ratios) gene counts using DESeq2 (*148*). We then tested for significant differences in gene expression between autumn and spring using a Wald test, followed by multiple testing correction on resulting p-values with the Benjamini and Hochberg procedure (*149*). Sex was used as an additional covariate (~sex + condition), but our design is imbalanced as not every season samples both sexes. Significantly differentially expressed genes were binned by fold change (>1.58 log-fold change), to quantify differentially expressed genes of high effect. Significant differentially expressed genes were also used to identify KEGG GO enrichment (*146*), and compared against the candidate list of genes with branch shift changes in expression to identify genes both plastic across seasons and consistent with expression adaptation in the shrew. To test if observed overlap was greater than expected by chance, we performed a Fisher's exact test.

Cell culture

Mustelo putoris furo (MPF) brain cells (ATCC, CRL-1656) were cultured in 10mL of Basal Medium Eagle (BME) supplemented with 14% sheep serum. Cells were cultured in 60.8-cm^2 treated tissue culture dishes at 37°C in 5% CO_2 atmosphere and 95% humidity. With induced cell death, cells were seeded into treated flat bottom six-well plates with 2mL/well of complete culture media.

Cell death induction

Three experiments were conducted to induce cell death in MPF cells (cold induced, peroxide induced, and heat induced), with only heat causing significant decrease in cell viability. *Cold induced*: Two 60.8-cm^2 tissue culture dishes of MPF cells were seeded into two six-well plates for 24 hours before reaching 80% confluency. In one experiment, "short cold" apoptosis was performed by immersing the six-well plate into a 0°C ice-water bath for 2 hours, followed by 3 hours of rewarming to 37°C in an incubator. Cells were then treated with crystal violet staining. In a similar experiment, "long cold" apoptosis was performed by immersing the six-well plate into a 0°C water bath for 4 hours, followed by 24 hours of rewarming to 37°C before crystal violet staining*Heat-induced cell death*: Two 60.8-cm^2 tissue culture dishes of MPF cells were seeded into two six-well plates for 24 hours before reaching 80% confluency. Heat cell death

was attempted by immersing the six-well plate into a 45°C water bath for 2 hours, followed by re-cooling to 37°C prior to crystal violet staining.

In vitro transcription and transfection of cells

The AmpliScribe T7 High Yield Transcription kit (Lucigen) was used for RNA in vitro transcription with a 2-hour incubation at 37°C using gblock sequences available in supplemental. BCL2L1 sequences were designed with a T7 promoter inserted at the beginning to facilitate transcription (Integrated DNA Technologies). We selected *BCL2L1* because it is the gene furthest downstream in the apoptotic pathway, thus making it the most directly involved gene in programmed cell death, whereas upstream genes could influence additional genes or alternative processes. RNA transcripts were purified using the Qiagen miRNA kit and concentration determined using a Nanodrop2000 (Thermo Fisher Scientific). Two 60.8-cm^2 tissue culture dishes of MPF cells were seeded into two six-well plates for 24 hours before reaching 80% confluency. 300ng of *BCL2L1* RNA or a scrambled form of *BCL2L1* RNA were transfected with Lipofectamine 3000 into each well for 24 hours according to manufacturer's instructions (Thermo Fisher Scientific). In short, two tubes were used to make a master mix for each RNA sample. Tube 1 contained 125µL/well of Opti-mem (Thermo Fisher Scientific) with 7.5 µL/well of Lipo3000. Tube 2 contained 125µL/well of Opti-mem, 5µL/well of P3000 and 300ng/well of RNA. Tube 2 was added to tube 1 and incubated 15 minutes at room temperature. The solution was then gently mixed and dispersed evenly to cells.

Crystal violet cell viability assays

Crystal violet solution was made using 500mg crystal violet powder in 100mL of 50% methanol. Cells were cultured to 80% confluency in two six-well plates. Complete media was aspirated in wells and washed three times in 1mL of 1X DPBS before 500µL of crystal violet solution was added to each well. Plates were wrapped in foil and placed on a shaker for 30 minutes. After time elapsed, crystal violet was removed, and cells were washed with tap water until free color was no longer visible. Plates were left at room temperature for 10-15 minutes until dry. 500µL of 100% methanol was added to each well and plates were put on a shaker for one hour at room temperature. 100µL of solution was taken from each well in triplicate and added to a 96-well plate. 100µL of 100% methanol was added in triplicate to a row for normalization of background absorbance. Wells were read at 570nm using a spectrophotometer (BioTek). For viability, data are reported as a percentage of control or optical density for absorbance. For statistical analysis, differences were judged to be statistically significant when $p<0.05$ by a Welch's two sample t-test.

Data Availability

Supplementary tables, data, results, and code deposited and found on Github https://github.com/wrthomas315/Sorex_Hypothalamus_Transcriptomics2. Raw sequencing data located in the NCBI Sequencing Read Archive (BioProject PRJNA941271). Supplemental Figures. S1–S2: DOI: https://doi.org/10.6084/m9.figshare.26049739.v1.

Grants

Human Frontiers of Science Program, award: RGP0013/2019 (to Dina K. N. Dechmann, John Nieland, Liliana M. Dávalos).

WRT was supported in part by a Stony Brook University Presidential Innovation and Excellence award to LMD.

Disclosures

Authors declare no competing interests.

Author Contributions

Conceptualization: DD RGH WRT
Methodology: ETO LMD RGH TAR WRT
Software: WRT
Validation: APC ETO
Formal analysis: APC ETO TAR WRT
Investigation: CB ETO TAR WRT
Resources: CB DD ETO RGH TAR
Data Curation: WRT
Writing – Original Draft: ETO TAR WRT
Writing – Review and Editing: APC CB DD DE ETO JDN LMD TAR
Visualization: ETO TAR WRT
Supervision: LMD RGH
Project administration: DD LMD
Funding acquisition: APC DD LMD JDN

Figure Legends

Figure 1 – (A) Hierarchical clustering of expression identified 12 distinct clusters, of which seven clusters (1, 4, 5, 6, 7, 9, 10) comprising of 394 genes, showed variation consistent with seasonality or Dehnel's phenomenon. **(B)** Functional characterization of these genes using KEGG GO pathways found an enrichment of 14 pathways ($p<0.05$), many of which have been implicated in hypothalamic control of homeostatic maintenance, including, relaxin signaling, neuroactive ligand-receptor interaction, HIF-1 signaling, and PI3K-Akt signaling.

Figure 2 – (A) Volcano plot of significant ($p_{adj}<0.05$) differentially expressed genes (colored) between phenotypic extremes of hypothalami size change (spring vs autumn) plotted by log fold-change. **(B)** Pathway enrichment analysis identified 15 pathways to be enriched for differentially expressed genes, including pathways in cancer and apoptosis (downregulated). **(C)** Patterning of gene expression across seasons of Dehnel's phenomenon for genes found in the cancer (all) and apoptosis (red) pathways, including *BCL2L1* (dashed). **(D)** Cell viability of *Mustela putorious furo* neural cell lines exposed to four treatments: scrambled *BCL2L1* overexpression, *BCL2L1* overexpression, heat with scrambled BCL2L1 overexpression, and heat with *BCL2L1* overexpression. Heat significantly reduced the cell viability compared to controls but was not rescued by *BCL2L1* overexpression.

Figure 3 – (A) Heatmap and boxplots of genes with shrew-specific upregulation compared to other mammals associated with processes including calcium signaling, autophagy, neurological functions, **(B)** metabolic homeostasis and environmental sensing.

Figure 4 - Boxplots of CCDC22 showing both evolutionary upregulation (**A**) in the shrew and differential expression between spring and autumn individuals, as found in three other genes (*KCNS1*, *LMX1A*, *PAQR4*) (**B**), which have been implicated in the development and progression of human neurological disorders.

Tables

Table 1 – Significant shrew-specific upregulation of genes associated with calcium signaling pathways, blood brain barrier plasticity, food intake and leptin response, and other related functions.

Gene	Function	FC	P-value	KEGG (p<0.05)
WNT7A	BBB/Neurogenesis/Angiogenesis	8.60	0.000	NA
MFSD2A	Transports DHA across blood brain barrier/Fasting induced	5.22	0.000	NA
SLC22A23	BBB plasticity	4.69	0.000	NA
VEGFA	BBB plasticity/Calcium Signaling	4.04	0.024	Calcium Signaling
CASQ1	Calcium Signaling/myopathy	7.22	0.000	Calcium Signaling
HRH2	Calcium Signaling/Sleep related/Histaminergic neurons	11.74	0.000	Calcium Signaling
TACR2	Calcium Signaling	14.21	0.000	Calcium Signaling
PPIF	Calcium Signaling	4.92	0.000	Calcium Signaling
SPHK2	Calcium Signaling/Food intake	3.18	0.025	Calcium Signaling
GRIN1	Calcium Signaling/Food intake	3.60	0.016	Calcium Signaling
FOXA2	Food intake	19.37	0.000	NA
SDC1	Food intake	10.74	0.000	NA
AGT	Leptin Response/Food Intake/FOXO1	4.23	0.029	NA
IRX5	Leptin response/Food intake/Neurogenesis	3.83	0.006	NA
GRB2	Leptin Response	3.36	0.003	NA
FOXO4	Leptin Response	5.99	0.000	NA
GPR3	Thermogenesis/Obesity	3.77	0.002	NA
KCNJ10	Metabolic homeostasis/Tanycyte formation	4.87	0.002	NA
ELOVL2	Lipid Metabolism/Elongation of VLFA	6.29	0.001	NA
MRPS6	Mitochondria protein synthesis/Parkinson's	4.00	0.000	NA
ATG101	Autophagy	3.95	0.000	Autophagy
ATG4D	Autophagy	3.84	0.000	Autophagy
MLST8	Autophagy/mTor pathway	8.03	0.000	Autophagy
LAMTOR3	Modulates mTor pathway	5.37	0.000	NA
SIRT7	Neuroprotective during neurogenesis	4.64	0.004	NA
HTRA2	Aging/Cell and organ size/Neuroprotection	3.86	0.000	NA
CCDC22	NF-KB Regulation/Ritscher-Schinzel	6.95	0.000	NA
RGS14	Suppressed synaptic plasticity (LTP)	6.21	0.002	NA
DLGAP3	OCD	5.72	0.001	NA
EMC8	Protein homeostasis of GABAnergic neurons/ER membrane complex	3.42	0.021	NA
RGS4	GABAnergic/Photoperiod/Environmental processing	6.81	0.002	NA
RBFOX3	Promotes sleep/Associated with epilepsy	7.10	0.000	NA
B4GALNT1	Ganglioside synthesis/Promotes BACE1	4.30	0.008	NA

Literature cited

1. M. Arain, M. Haque, L. Johal, P. Mathur, W. Nel, A. Rais, R. Sandhu, S. Sharma, Maturation of the adolescent brain. *Neuropsychiatr. Dis. Treat.* **9**, 449–461 (2013).
2. S. J. Gould, Allometry and size in ontogeny and phylogeny. *Biol. Rev. Camb. Philos. Soc.* **41**, 587–640 (1966).
3. J. Lázaro, M. Hertel, M. Muturi, D. K. N. Dechmann, Seasonal reversible size changes in the braincase and mass of common shrews are flexibly modified by environmental conditions. *Sci. Rep.* **9**, 1–10 (2019).
4. Z. Pucek, Seasonal and age change in shrews as an adaptive process. *Symp. zool. Soc. Lond.* **26**, 189–207 (1970).
5. M. Pucek, Water contents and seasonal changes of the brain-weight in shrews. *Acta Theriol. (Warsz).* **10**, 353–367 (1965).
6. Z. Pucek, Seasonal and age changes in the weight of internal organs of shrews. *Acta Theriol. (Warsz).* **10**, 369–438 (1965).
7. L. Keicher, M. T. O'Mara, C. C. Voigt, D. K. N. Dechmann, Stable carbon isotopes in breath reveal fast metabolic incorporation rates and seasonally variable but rapid fat turnover in the common shrew (Sorex araneus). *J. Exp. Biol.* **220**, 2834–2841 (2017).
8. S. Churchfield, L. Rychlik, J. R. E. Taylor, Food resources and foraging habits of the common shrew, Sorex araneus: Does winter food shortage explain Dehnel's phenomenon? *Oikos*. **121**, 1593–1602 (2012).
9. J. R. E. Taylor, L. Rychlik, S. Churchfield, Winter reduction in body mass in a very small, nonhibernating mammal: Consequences for heat loss and metabolic rates. *Physiol. Biochem. Zool.* **86**, 9–18 (2013).
10. H. Hyvärinen, Wintering strategy of voles and shrews in Findland. *Winter Ecol. Small Mamm.* **10**, 139–148 (1984).
11. P. J. Schaeffer, M. T. O'Mara, J. Breiholz, L. Keicher, J. Lázaro, M. Muturi, D. K. N. Dechmann, Metabolic rate in common shrews is unaffected by temperature, leading to lower energetic costs through seasonal size reduction. *R. Soc. Open Sci.* **7** (2020), doi:10.1098/rsos.191989.
12. W. R. Thomas, D. K. N. Dechmann, J. Nieland, C. Baldoni, D. Carlson, D. Von Elverfeldt, J. Holm-jacobsen, M. Muturi, A. Corthals, M. Liliana, Molecular mechanisms of seasonal brain shrinkage and regrowth in Sorex araneus. *bioRxiv*, 1–16 (2023).
13. G. G. Auteri, L. L. Knowles, Decimated little brown bats show potential for adaptive change. *Sci. Rep.* **10**, 1–10 (2020).
14. F. Geiser, Ontogeny and phylogeny of endothermy and torpor in mammals and birds. *Comp. Biochem. Physiol. - A Mol. Integr. Physiol.* **150**, 176–180 (2008).
15. E. Ferris, C. Gregg, Parallel Accelerated Evolution in Distant Hibernators Reveals Candidate Cis Elements and Genetic Circuits Regulating Mammalian Obesity. *Cell Rep.* **29**, 2608–2620 (2019).
16. C. Turbill, C. Bieber, T. Ruf, Hibernation is associated with increased survival and the evolution of slow life histories among mammals. *Proc. R. Soc. B Biol. Sci.* **278**, 3355–3363 (2011).
17. S. L. Faherty, J. Luis Villanueva-Cañas, P. H. Klopfer, M. M. Albà, A. D. Yoder, Gene expression profiling in the hibernating primate, Cheirogaleus medius. *Genome Biol. Evol.* **8**, 2413–2426 (2016).
18. J. L. Villanueva-Cañas, S. L. Faherty, A. D. Yoder, M. M. Albà, Comparative genomics of mammalian hibernators using gene networks. *Integr. Comp. Biol.* **54**, 452–462 (2014).
19. M. Genoud, K. Isler, R. D. Martin, Comparative analyses of basal rate of metabolism in mammals□: data selection does matter. *Biol. Rev.* **93**, 404–438 (2018).
20. J. R. E. Taylor, "Evolution of Energetic Strategies in Shrews" in *Evolution of Shrews* (1998), pp. 309–346.
21. J. B. Searle, J. Zima, P. D. Polly, *Shrews, Chromosomes and Speciation* (Cambridge University Press, Cambridge, 2019).

22. K. Healy, T. Guillerme, S. Finlay, A. Kane, S. B. A. Kelly, D. McClean, D. J. Kelly, I. Donohue, A. L. Jackson, N. Cooper, Ecology and mode-of-life explain lifespan variation in birds and mammals. *Proc. R. Soc. B*. **281** (2014), doi:10.1098/rspb.2014.0298.
23. P. Mergenthaler, U. Lindauer, G. A. Dienel, A. Meisel, Sugar for the brain: The role of glucose in physiological and pathological brain function. *Trends Neurosci.* **36**, 587–597 (2013).
24. S. Via, R. Lande, Genotype-environment interaction and the evolution of phenotypic plasticity. *Evolution (N. Y).* **39**, 505–522 (1985).
25. C. J. Brauer, P. J. Unmack, L. B. Beheregaray, Comparative ecological transcriptomics and the contribution of gene expression to the evolutionary potential of a threatened fish. *Mol. Ecol.* **26**, 6841–6856 (2017).
26. M. A. Bernal, C. Schunter, R. Lehmann, D. J. Lightfoot, B. J. M. Allan, H. D. Veilleux, J. L. Rummer, P. L. Munday, T. Ravasi, Species-specific molecular responses of wild coral reef fishes during a marine heatwave. *Sci. Adv.* **6**, 1–12 (2020).
27. D. B. Stern, K. A. Crandall, The evolution of gene expression underlying vision loss in cave animals. *Mol. Biol. Evol.* **35**, 2005–2014 (2018).
28. G. B. Gillard, L. Grønvold, L. L. Røsæg, M. M. Holen, Ø. Monsen, B. F. Koop, E. B. Rondeau, M. K. Gundappa, J. Mendoza, D. J. Macqueen, R. V. Rohlfs, S. R. Sandve, T. R. Hvidsten, Comparative regulomics supports pervasive selection on gene dosage following whole genome duplication. *Genome Biol.* **22**, 1–18 (2021).
29. G. C. Conant, The lasting after-effects of an ancient polyploidy on the genomes of teleosts. *PLoS One*. **15**, 1–26 (2020).
30. I. Braasch, A. R. Gehrke, J. J. Smith, K. Kawasaki, T. Manousaki, J. Pasquier, A. Amores, T. Desvignes, P. Batzel, J. Catchen, A. M. Berlin, M. S. Campbell, D. Barrell, K. J. Martin, J. F. Mulley, V. Ravi, A. P. Lee, T. Nakamura, D. Chalopin, S. Fan, D. Wcisel, C. Caestro, J. Sydes, F. E. G. Beaudry, Y. Sun, J. Hertel, M. J. Beam, M. Fasold, M. Ishiyama, J. Johnson, S. Kehr, M. Lara, J. H. Letaw, G. W. Litman, R. T. Litman, M. Mikami, T. Ota, N. R. Saha, L. Williams, P. F. Stadler, H. Wang, J. S. Taylor, Q. Fontenot, A. Ferrara, S. M. J. Searle, B. Aken, M. Yandell, I. Schneider, J. A. Yoder, J. N. Volff, A. Meyer, C. T. Amemiya, B. Venkatesh, P. W. H. Holland, Y. Guiguen, J. Bobe, N. H. Shubin, F. Di Palma, J. Alföldi, K. Lindblad-Toh, J. H. Postlethwait, The spotted gar genome illuminates vertebrate evolution and facilitates human-teleost comparisons. *Nat. Genet.* **48**, 427–437 (2016).
31. S. Lien, B. F. Koop, S. R. Sandve, J. R. Miller, M. P. Kent, T. Nome, T. R. Hvidsten, J. S. Leong, D. R. Minkley, A. Zimin, F. Grammes, H. Grove, A. Gjuvsland, B. Walenz, R. A. Hermansen, K. Von Schalburg, E. B. Rondeau, A. Di Genova, J. K. A. Samy, J. Olav Vik, M. D. Vigeland, L. Caler, U. Grimholt, S. Jentoft, D. Inge Våge, P. De Jong, T. Moen, M. Baranski, Y. Palti, D. R. Smith, J. A. Yorke, A. J. Nederbragt, A. Tooming-Klunderud, K. S. Jakobsen, X. Jiang, D. Fan, Y. Hu, D. A. Liberles, R. Vidal, P. Iturra, S. J. M. Jones, I. Jonassen, A. Maass, S. W. Omholt, W. S. Davidson, The Atlantic salmon genome provides insights into rediploidization. *Nature*. **533**, 200–205 (2016).
32. S. R. Sandve, R. V. Rohlfs, T. R. Hvidsten, Subfunctionalization versus neofunctionalization after whole-genome duplication. *Nat. Genet.* **50**, 908–909 (2018).
33. T. F. Rogers, D. H. Palmer, A. E. Wright, Sex-Specific Selection Drives the Evolution of Alternative Splicing in Birds. *Mol. Biol. Evol.* **38**, 519–530 (2021).
34. R. V. Rohlfs, R. Nielsen, Phylogenetic ANOVA: The expression variance and evolution model for quantitative trait evolution. *Syst. Biol.* **64**, 695–708 (2015).
35. J. Chen, R. Swofford, J. Johnson, B. B. Cummings, N. Rogel, K. Lindblad-Toh, W. Haerty, F. di Palma, A. Regev, A quantitative model for characterizing the evolutionary history of mammalian gene expression. *bioRxiv*, 53–63 (2017).
36. E. Yapar, E. Saglican, H. M. Dönertaş, E. Özkurt, Z. Yan, H. Hu, S. Guo, B. Erdem, R. V. Rohlfs, P. Khaitovich, M. Somel, Convergent evolution of primate testis transcriptomes reflects mating strategy. *bioRxiv*, 1–25 (2021).

37. E. Sjöstedt, W. Zhong, L. Fagerberg, M. Karlsson, N. Mitsios, C. Adori, P. Oksvold, F. Edfors, A. Limiszewska, F. Hikmet, J. Huang, Y. Du, L. Lin, Z. Dong, L. Yang, X. Liu, H. Jiang, X. Xu, J. Wang, H. Yang, L. Bolund, A. Mardinoglu, C. Zhang, K. Von Feilitzen, C. Lindskog, F. Pontén, Y. Luo, T. Hökfelt, M. Uhlén, J. Mulder, An atlas of the protein-coding genes in the human, pig, and mouse brain. *Science (80-.).* **367**, 1–16 (2020).
38. J. Lázaro, M. Hertel, C. C. Sherwood, M. Muturi, D. K. N. Dechmann, Profound seasonal changes in brain size and architecture in the common shrew. *Brain Struct. Funct.* **223**, 2823–2840 (2018).
39. M. E. Pamenter, Adaptations to a hypoxic lifestyle in naked mole-rats. *J. Exp. Biol.* **225** (2022), doi:10.1242/jeb.196725.
40. M. O. Dietrich, T. L. Horvath, Hypothalamic control of energy balance: Insights into the role of synaptic plasticity. *Trends Neurosci.* **36**, 65–73 (2013).
41. S. Ramón y Cajal, Sur la fine structure du lobe optique des oiseaux et sur l'origine réelle des nerfs optiques. *J. Int. Anat. Physiol.* **7**, 1–30 (1891).
42. R. Apfelbach, D. Kruska, Postnatal development of the brain of the ferret Mustela putorius F Furo (Mustelidae, Mammalia). *Int. J. Mamm. Biol.* **44**, 127–131 (1979).
43. A. Singla, A. Fedoseienko, S. S. P. Giridharan, B. L. Overlee, A. Lopez, D. Jia, J. Song, K. Huff-Hardy, L. Weisman, E. Burstein, D. D. Billadeau, Endosomal PI(3)P regulation by the COMMD/CCDC22/CCDC93 (CCC) complex controls membrane protein recycling. *Nat. Commun.* **10** (2019), doi:10.1038/s41467-019-12221-6.
44. E. J. Hoekstra, L. von Oerthel, L. P. van der Heide, W. M. Kouwenhoven, J. V. Veenvliet, I. Wever, Y. R. Jin, J. K. Yoon, A. J. A. van der Linden, F. C. P. Holstege, M. J. Groot Koerkamp, M. P. Smidt, Lmx1a Encodes a Rostral Set of Mesodiencephalic Dopaminergic Neurons Marked by the Wnt/B-Catenin Signaling Activator R-spondin 2. *PLoS One*. **8**, 1–12 (2013).
45. C. Tsantoulas, F. Denk, M. Signore, M. A. Nassar, K. Futai, S. B. McMahon, Mice lacking Kcns1 in peripheral neurons show increased basal and neuropathic pain sensitivity. *Pain*. **159**, 1641–1651 (2018).
46. L. Pedersen, P. Panahandeh, M. I. Siraji, S. Knappskog, P. E. Lønning, R. Gordillo, P. E. Scherer, A. Molven, K. Teigen, N. Halberg, Golgi-localized PAQR4 mediates antiapoptotic ceramidase activity in breast cancer. *Cancer Res.* **80**, 2163–2174 (2020).
47. B. M. C. McGowan, S. A. Stanley, M. A. Ghatei, S. R. Bloom, "Relaxin-3 and its role in neuroendocrine function" in *Annals of the New York Academy of Sciences* (2009), vol. 1160, pp. 250–255.
48. C. M. Smith, P. J. Ryan, I. T. Hosken, S. Ma, A. L. Gundlach, Relaxin-3 systems in the brain — The first 10 years. *J. Chem. Neuroanat. jo*. **42**, 262–275 (2011).
49. H. Otsubo, T. Onaka, H. Suzuki, A. Katoh, T. Ohbuchi, M. Todoroki, M. Kobayashi, H. Fujihara, T. Yokoyama, T. Matsumoto, Y. Ueta, Centrally administered relaxin-3 induces Fos expression in the osmosensitive areas in rat brain and facilitates water intake. *Peptides*. **31**, 1124–1130 (2010).
50. B. M. C. McGowan, S. A. Stanley, K. L. Smith, N. E. White, M. M. Connolly, E. L. Thompson, J. V. Gardiner, K. G. Murphy, M. A. Ghatei, S. R. Bloom, Central relaxin-3 administration causes hyperphagia in male wistar rats. *Endocrinology*. **146**, 3295–3300 (2005).
51. C. Lenglos, A. Mitra, G. Guèvremont, E. Timofeeva, Sex differences in the effects of chronic stress and food restriction on body weight gain and brain expression of CRF and relaxin-3 in rats. *Genes, Brain Behav.* **12**, 370–387 (2013).
52. C. De Ávila, S. Chometton, C. Lenglos, J. Calvez, A. L. Gundlach, E. Timofeeva, Differential effects of relaxin-3 and a selective relaxin-3 receptor agonist on food and water intake and hypothalamic neuronal activity in rats. *Behav. Brain Res.* **336**, 135–144 (2018).
53. J. Calvez, C. Lenglos, C. de Ávila, G. Guèvremont, E. Timofeeva, Differential effects of central administration of relaxin-3 on food intake and hypothalamic neuropeptides in male and female rats. *Genes, Brain Behav.* **14**, 550–563 (2015).
54. C. Lenglos, J. Calvez, E. Timofeeva, Sex-specific effects of relaxin-3 on food intake and brain expression of corticotropin-releasing factor in rats. *Endocrinology*. **156**, 523–533 (2015).

55. B. M. C. McGowan, S. A. Stanley, N. E. White, A. Spangeus, M. Patterson, E. L. Thompson, K. L. Smith, J. Donovan, J. V. Gardiner, M. A. Ghatei, S. R. Bloom, Hypothalamic mapping of orexigenic action and Fos-like immunoreactivity following relaxin-3 administration in male Wistar rats. *Am. J. Physiol. - Endocrinol. Metab.* **292**, 913–919 (2007).
56. N. Ahmad, W. Wang, R. Nair, S. Kapila, Relaxin induces matrix-metalloproteinases-9 and -13 via RXFP1: Induction of MMP-9 involves the PI3K, ERK, Akt and PKC-ζ pathways. *Mol. Cell. Endocrinol.* **363**, 46–61 (2012).
57. C. W. Dessauer, B. T. Nguyen, Relaxin stimulates multiple signaling pathways: Activation of cAMP, PI3K, and PKCζ in THP-1 cells. *Ann. N. Y. Acad. Sci.* **1041**, 272–279 (2005).
58. L. Shen, D. Q. Wang, P. Tso, R. J. Jandacek, S. C. Woods, M. Liu, Physiology & Behavior Apolipoprotein E reduces food intake via PI3K / Akt signaling pathway in the hypothalamus. *Physiol. Behav.* **105**, 124–128 (2011).
59. L. Shen, C. C. Lo, L. A. Woollett, M. Liu, Biochemical and Biophysical Research Communications Apolipoprotein A-IV exerts its anorectic action through a PI3K / Akt signaling pathway in the hypothalamus. *Biochem. Biophys. Res. Commun.* **494**, 152–157 (2017).
60. K. D. Niswender, G. J. Morton, W. H. Stearns, C. J. Rhodes, M. G. Myers, M. W. Schwartz, Intracellular signalling: Key enzyme in leptin-induced anorexia. *Nature*. **413**, 794–795 (2001).
61. A. C. Könner, R. Janoschek, L. Plum, S. D. Jordan, E. Rother, X. Ma, C. Xu, P. Enriori, B. Hampel, G. S. Barsh, C. R. Kahn, M. A. Cowley, F. M. Ashcroft, J. C. Brüning, Insulin Action in AgRP-Expressing Neurons Is Required for Suppression of Hepatic Glucose Production. *Cell Metab.* **5**, 438–449 (2007).
62. J. W. Hill, Y. Xu, F. Preitner, M. Fukuda, Y. R. Cho, J. Luo, N. Balthasar, R. Coppari, L. C. Cantley, B. B. Kahn, J. J. Zhao, J. K. Elmquist, Phosphatidyl inositol 3-kinase signaling in hypothalamic proopiomelanocortin neurons contributes to the regulation of glucose homeostasis. *Endocrinology*. **150**, 4874–4882 (2009).
63. J. Karar, A. Maity, PI3K/AKT/mTOR Pathway in Angiogenesis. *Front. Mol. Neurosci.* **4**, 1–8 (2011).
64. A. Maity, N. Pore, J. Lee, D. Solomon, D. onald M. O'Rourke, Epidermal growth factor receptor transcriptionally up-regulates vascular endothelial growth factor expression in human glioblastoma cells via a pathway involving phosphatidylinositol 3'-kinase and distinct from that induced by hypoxia. *Cancer Res.* **60**, 5879–5886 (2000).
65. C. M. Taniguchi, B. Emanuelli, C. R. Kahn, Critical nodes in signalling pathways: insights into insulin action. *Nat. Rev. Mol. Cell Biol.* **7**, 85–96 (2006).
66. Z. Li, X. Liu, P. Zhang, R. Han, G. Sun, R. Jiang, Y. Wang, X. Liu, Comparative transcriptome analysis of hypothalamus-regulated feed intake induced by exogenous visfatin in chicks. *BMC Genomics*. **19**, 1–17 (2018).
67. B. Chen, W. Fang, Y. Li, T. Xiong, M. Zhou, L. Wan, Q. Liu, W. Zhang, X. Hu, H. Mao, S. Liu, RNA-seq and differential expression analysis of the duck transcriptome□: The effect of short-term cage-rearing. *bioRxiv* (2021), doi:https://doi.org/10.1101/2021.05.13.444049.
68. J.-M. Kim, K.-S. Lim, M. Byun, K.-T. Lee, Y.-R. Yang, M. Park, D. Lim, H.-H. Chai, H.-T. Bang, J. Hwangbo, Y.-H. Choi, Y.-M. Cho, J.-E. Park, Identification of the acclimation genes in transcriptomic responses to heat stress of White Pekin duck. *Cell Stress Chaperones*. **22**, 787–797 (2017).
69. X. Y. Chen, R. Li, M. Wang, Z. Y. Geng, Identification of differentially expressed genes in hypothalamus of chicken during cold stress. *Miol Biol Rep*. **41**, 2243–2248 (2014).
70. S. Raab, H. Beck, A. Gaumann, A. Yüce, H. P. Gerber, K. Plate, H. P. Hammes, N. Ferrara, G. Breier, Impaired brain angiogenesis and neuronal apoptosis induced by conditional homozygous inactivation of vascular endothelial growth factor. *Thromb. Haemost.* **91**, 595–605 (2004).
71. P. Carmeliet, V. Ferreira, G. Breier, S. Pollefeyt, L. Kieckens, M. Gertsenstein, M. Fahrig, A. Vandenhoeck, K. Harpal, C. Eberhardt, C. Declercq, J. Pawling, L. Moons, D. Collen, W. Risau, A. Nagy, Abnormal blood vessel development and lethality in embryos lacking a single vascular

endothelial growth factor allele. *Nature*. **380**, 435–439 (1996).
72. R. Daneman, D. Agalliu, L. Zhou, F. Kuhnert, C. J. Kuo, B. A. Barres, Wnt/β-catenin signaling is required for CNS, but not non-CNS, angiogenesis. *Proc. Natl. Acad. Sci. U. S. A.* **106**, 641–646 (2009).
73. A. T. Argaw, L. Asp, J. Zhang, K. Navrazhina, T. Pham, J. N. Mariani, S. Mahase, D. J. Dutta, J. Seto, E. G. Kramer, N. Ferrara, M. V. Sofroniew, G. R. John, Astrocyte-derived VEGF-A drives blood-brain barrier disruption in CNS inflammatory disease. *J. Clin. Invest.* **122**, 2454–2468 (2012).
74. H. Kim, J. M. Lee, J. S. Park, S. A. Jo, Y. O. Kim, C. W. Kim, I. Jo, Dexamethasone coordinately regulates angiopoietin-1 and VEGF: A mechanism of glucocorticoid-induced stabilization of blood-brain barrier. *Biochem. Biophys. Res. Commun.* **372**, 243–248 (2008).
75. A. T. Argaw, B. T. Gurfein, Y. Zhang, A. Zameer, G. R. John, VEGF-mediated disruption of endothelial CLN-5 promotes blood-brain barrier breakdown. *Proc. Natl. Acad. Sci. U. S. A.* **106**, 1977–1982 (2009).
76. G. Lan, P. Wang, R. B. Chan, Z. Liu, Z. Yu, X. Liu, Y. Yang, J. Zhang, Astrocytic VEGFA: An essential mediator in blood–brain-barrier disruption in Parkinson's disease. *Glia*. **70**, 337–353 (2022).
77. B. Obermeier, R. Daneman, R. M. Ransohoff, Development, maintenance and disruption of the blood-brain barrier. *Nat. Med.* **19**, 1584–1596 (2013).
78. L. Bennett, M. Yang, G. Enikolopov, L. Iacovitti, Circumventricular organs: A novel site of neural stem cells in the adult brain. *Mol. Cell. Neurosci.* **41**, 337–347 (2009).
79. F. Langlet, B. E. Levin, S. Luquet, M. Mazzone, A. Messina, A. A. Dunn-Meynell, E. Balland, A. Lacombe, D. Mazur, P. Carmeliet, S. G. Bouret, V. Prevot, B. Dehouck, Tanycytic VEGF-A boosts blood-hypothalamus barrier plasticity and access of metabolic signals to the arcuate nucleus in response to fasting. *Cell Metab.* **17**, 607–617 (2013).
80. R. Haddad-Tóvolli, N. R. V. Dragano, A. F. S. Ramalho, L. A. Velloso, Development and function of the blood-brain barrier in the context of metabolic control. *Front. Neurosci.* **11**, 1–12 (2017).
81. T. K. T. Lam, G. J. Schwartz, L. Rossetti, Hypothalamic sensing of fatty acids. *Nat. Neurosci.* **8**, 579–584 (2005).
82. P.-M. Chevillard, M. Batailler, B. Piégu, A. Estienne, M.-C. Blache, J.-P. Dubois, D. Pillon, P. Vaudin, J. Dupont, N. Just, M. Migaud, Seasonal vascular plasticity in the mediobasal hypothalamus of the adult ewe. *Histochem. Cell Biol.* **157**, 581–593 (2022).
83. J. Castle-Miller, D. O. Bates, D. J. Tortonese, Mechanisms regulating angiogenesis underlie seasonal control of pituitary function. *Proc. Natl. Acad. Sci. U. S. A.* **114**, E2514–E2523 (2017).
84. A. Tabecka-Lonczynska, J. Mytych, P. Solek, A. Abrachamowicz, M. Welz, M. Koziorowski, Local regulators of seasonal reproduction processes in uterus masculinus of an adult male european bison (bison bonasus, linnaeus 1758). *J. Physiol. Pharmacol.* **69**, 747–753 (2018).
85. Y. Yao, W. Xie, D. Chen, Y. Han, Z. Yuan, H. Zhang, Q. Weng, Seasonal expressions of VEGF and its receptors VEGFR1 and VEGFR2 in the prostate of the wild ground squirrels (Spermophilus dauricus). *Eur. J. Histochem.* **65**, 35219 (2021).
86. W. Ma, G. Fuentes, X. Shi, C. Verma, G. K. Radda, W. Han, FoxO1 negatively regulates leptin-induced POMC transcription through its direct interaction with STAT3. *Biochem. J.* **466**, 291–298 (2015).
87. M. Amitani, A. Asakawa, H. Amitani, A. Inui, The role of leptin in the control of insulin-glucose axis. *Front. Neurosci.* **7**, 1–12 (2013).
88. T. Sasaki, H. J. Kim, M. Kobayashi, Y. I. Kitamura, H. Yokota-Hashimoto, T. Shiuchi, Y. Minokoshi, T. Kitamura, Induction of hypothalamic Sirt1 leads to cessation of feeding via agouti-related peptide. *Endocrinology*. **151**, 2556–2566 (2010).
89. J. Nakae, Y. Cao, H. Daitoku, A. Fukamizu, W. Ogawa, Y. Yano, Y. Hayashi, The LXXLL motif of murine forkhead transcription factor FoxO1 mediates Sirt1-dependent transcriptional activity. *J.*

Clin. Invest. **116**, 2473–2483 (2006).
90. B. Wang, J. Zhu, K. Mounzih, E. F. Chehab, Y. Ke, F. F. Chehab, Overexpression of the transcription factor foxo4 is associated with rapid glucose clearance. *Mol. Cell. Endocrinol.* **307**, 217–223 (2009).
91. M. B. Ahrens, M. B. Orger, D. N. Robson, J. M. Li, P. J. Keller, Whole-brain functional imaging at cellular resolution using light-sheet microscopy. *Nat. Methods*. **10**, 413–420 (2013).
92. K. Mann, C. L. Gallen, T. R. Clandinin, Whole-Brain Calcium Imaging Reveals an Intrinsic Functional Network in Drosophila. *Curr. Biol.* **27**, 2389–2396 (2017).
93. S. B. Kater, M. P. Mattson, C. Cohan, J. Connor, Calcium regulation of the neuronal growth cone. *Trends Neurosci.* **11**, 315–321 (1988).
94. M. P. Mattson, Neurotransmitters in the regulation of neuronal cytoarchitecture. *Brain Res. Rev.* **472**, 179–212 (1988).
95. K. Deisseroth, H. Bito, R. W. Tsien, Signaling from synapse to nucleus: Postsynaptic CREB phosphorylation during multiple forms of hippocampal synaptic plasticity. *Neuron*. **16**, 89–101 (1996).
96. H. Bito, K. Deisseroth, R. W. Tsien, Ca2+-dependent regulation in neuronal gene expression. *Curr. Opin. Neurobiol.* **7**, 419–429 (1997).
97. M. J. Berridge, Neuronal calcium. *Neuron*. **21**, 13–26 (1998).
98. S. J. Zhang, M. Zou, L. Lu, D. Lau, D. A. W. Ditzel, C. Delucinge-Vivier, Y. Aso, P. Descombes, H. Bading, Nuclear calcium signaling controls expression of a large gene pool: Identification of a gene program for acquired neuroprotection induced by synaptic activity. *PLoS Genet.* **5** (2009), doi:10.1371/journal.pgen.1000604.
99. L. Redmond, A. Ghosh, Regulation of dendritic development by calcium signaling. *Cell Calcium*. **37**, 411–416 (2005).
100. C. Lohmann, R. O. L. Wong, Regulation of dendritic growth and plasticity by local and global calcium dynamics. *Cell Calcium*. **37**, 403–409 (2005).
101. H. Kazama, A. Nose, T. Morimoto-Tanifuji, Synaptic components necessary for retrograde signaling triggered by calcium/calmodulin-dependent protein kinase II during synaptogenesis. *Neuroscience*. **145**, 1007–1015 (2007).
102. C. Verderio, S. Coco, G. Fumagalli, M. Matteoli, Spatial changes in calcium signaling during the establishment of neuronal polarity and synaptogenesis. *J. Cell Biol.* **126**, 1527–1536 (1994).
103. K. Michaelsen, C. Lohmann, Calcium dynamics at developing synapses: Mechanisms and functions. *Eur. J. Neurosci.* **32**, 218–223 (2010).
104. R. C. Malenka, J. A. Kauer, R. S. Zucker, R. A. Nicoll, Postsynaptic Calcium Is Sufficient for Potentiation of Hippocampal Synaptic Transmission. *Science (80-.).* **242**, 81–84 (1988).
105. S. Poser, D. R. Storm, Role of Ca2+-stimulated adenylyl cyclases in LTP and memory formation. *Int. J. Dev. Neurosci.* **19**, 387–394 (2001).
106. D. M. Wilson, M. R. Cookson, L. Van Den Bosch, H. Zetterberg, D. M. Holtzman, I. Dewachter, Hallmarks of neurodegenerative diseases. *Cell*. **186**, 693–714 (2023).
107. B. Smith, thesis, Max Planck Institute for Ornithology (2016).
108. N. T. Bui, A. Livolsi, J. F. Peyron, J. H. M. Prehn, Activation of nuclear factor κB and bcl-x survival gene expression by nerve growth factor requires tyrosine phosphorylation of IκBα. *J. Cell Biol.* **152**, 753–763 (2001).
109. N. Motoyama, F. Wang, K. A. Roth, H. Sawa, K. Nakayama, I. Negishi, S. Senju, Q. Zhang, S. Fujii, D. Y. Loh, N. Motoyama, F. Wang, K. A. Roth, H. Sawa, K. Nakayama, K. Nakayama, I. Negishi, S. Senju, Q. Zhang, S. Fujii, D. Y. Loht, Massive Cell Death of Immature Hematopoietic Cells and Neurons in Bcl-x-Deficient Mice. *Science (80-.).* **267**, 1506–1510 (1995).
110. L. H. Boise, C. B. Thompson, Bcl-XL can inhibit apoptosis in cells that have undergone Fas-induced protease activation. *Proc. Natl. Acad. Sci. U. S. A.* **94**, 3759–3764 (1997).
111. C. C. Fleck, H. V. Carey, Modulation of apoptotic pathways in intestinal mucosa during hibernation. *Am. J. Physiol. - Regul. Integr. Comp. Physiol.* **289**, 586–595 (2005).

112. S. M. Logan, S. N. Tessier, J. Tye, K. B. Storey, Response of the JAK-STAT pathway to mammalian hibernation in 13-lined ground squirrel striated muscle. *Mol. Cell. Biochem.* **414**, 115–127 (2016).
113. A. N. Rouble, J. Hefler, H. Mamady, K. B. Storey, S. N. Tessier, Anti-apoptotic signaling as a cytoprotective mechanism in mammalian hibernation. *PeerJ*. **2013**, 1–21 (2013).
114. D. A. Guertin, D. M. Stevens, C. C. Thoreen, A. A. Burds, N. Y. Kalaany, J. Moffat, M. Brown, K. J. Fitzgerald, D. M. Sabatini, Ablation in Mice of the mTORC Components raptor, rictor, or mLST8 Reveals that mTORC2 Is Required for Signaling to Akt-FOXO and PKCα, but Not S6K1. *Dev. Cell*. **11**, 859–871 (2006).
115. R. A. Saxton, D. M. Sabatini, mTOR Signaling in Growth, Metabolism, and Disease. *Cell*. **168**, 960–976 (2017).
116. C. P. Baines, R. A. Kaiser, N. H. Purcell, N. S. Blair, H. Osinska, M. A. Hambleton, E. W. Brunskill, M. R. Sayen, R. A. Gottlieb, G. W. Dorn, J. Robbins, J. D. Molkentin, Loss of cyclophilin D reveals a critical role for mitochondrial permeability transition in cell death. *Nature*. **434**, 984–984 (2004).
117. Takashi Nakagawa, Shigeomi Shimizu, Tetsuya Watanabe, Osamu Yamaguchi, Kinya Otsu, Hirotaka Yamagata, Hidenori Inohara, Takeshi Kubo, Yoshihide Tsujimoto, Cyclophilin D-dependentmitochondrial permeabilitytransition regulates some necroticbut not apoptotic cell death. *Nature*. **434**, 648–652 (2005).
118. V. Li, T. Brustovetsky, N. Brustovetsky, Role of cyclophilin D-dependent mitochondrial permeability transition in glutamate-induced calcium deregulation and excitotoxic neuronal death. *Exp. Neurol.* **218**, 171–182 (2009).
119. A. P. Halestrap, A pore way to die. *Nature*. **430**, 984–984 (2004).
120. M. Maceyka, H. Sankala, N. C. Hait, H. Le Stunff, H. Liu, R. Toman, C. Collier, M. Zhang, L. S. Satin, A. H. Merrill, S. Milstien, S. Spiegel, SphK1 and SphK2, sphingosine kinase isoenzymes with opposing functions in sphingolipid metabolism. *J. Biol. Chem.* **280**, 37118–37129 (2005).
121. H. Liu, R. E. Toman, S. K. Goparaju, M. Maceyka, V. E. Nava, H. Sankala, S. G. Payner, M. Bektas, I. Ishii, J. Chun, S. Milstien, S. Spiegel, Sphingosine kinase type 2 is a putative BH3-only protein that induces apoptosis. *J. Biol. Chem.* **278**, 40330–40336 (2003).
122. J. F. Moruno-Manchon, N. E. Uzor, M. P. Blasco-Conesa, S. Mannuru, N. Putluri, E. E. Furr-Stimming, A. S. Tsvetkov, Inhibiting sphingosine kinase 2 mitigates mutant Huntingtin-induced neurodegeneration in neuron models of Huntington disease. *Hum. Mol. Genet.* **26**, 1305–1317 (2017).
123. N. Takasugi, T. Sasaki, K. Suzuki, S. Osawa, H. Isshiki, Y. Hori, N. Shimada, T. Higo, S. Yokoshima, T. Fukuyama, V. M. Y. Lee, J. Q. Trojanowski, T. Tomita, T. Iwatsubo, BACE1 activity is modulated by cell-associated sphingosine-1-phosphate. *J. Neurosci.* **31**, 6850–6857 (2011).
124. H. Du, L. Guo, F. Fang, D. Chen, A. A Sosunov, G. M McKhann, Y. Yan, C. Wang, H. Zhang, J. D. Molkentin, F. J. Gunn-Moore, J. P. Vonsattel, O. Arancio, J. X. Chen, S. Du Yan, Cyclophilin D deficiency attenuates mitochondrial and neuronal perturbation and ameliorates learning and memory in Alzheimer's disease. *Nat. Med.* **14**, 1097–1105 (2008).
125. H. Du, L. Guo, W. Zhang, M. Rydzewska, S. Yan, Cyclophilin D deficiency improves mitochondrial function and learning/memory in aging Alzheimer disease mouse model. *Neurobiol. Aging*. **32**, 398–406 (2011).
126. I. Voineagu, L. Huang, K. Winden, M. Lazaro, E. Haan, J. Nelson, J. McGaughran, L. S. Nguyen, K. Friend, A. Hackett, M. Field, J. Gecz, D. Geschwind, CCDC22: A novel candidate gene for syndromic X-linked intellectual disability. *Mol. Psychiatry*. **17**, 4–7 (2012).
127. M. Kolanczyk, P. Krawitz, J. Hecht, A. Hupalowska, M. Miaczynska, K. Marschner, C. Schlack, D. Emmerich, K. Kobus, U. Kornak, P. N. Robinson, B. Plecko, G. Grangl, S. Uhrig, S. Mundlos, D. Horn, Missense variant in CCDC22 causes X-linked recessive intellectual disability with features of Ritscher-Schinzel/3C syndrome. *Eur. J. Hum. Genet.* **23**, 633–638 (2015).

128. S. Neri, N. Maia, A. M. Fortuna, J. Damasio, E. Coale, M. Willis, P. Jorge, A. F. Højte, C. D. Fenger, R. S. Møller, A. Bayat, Expanding the pre- and postnatal phenotype of WASHC5 and CCDC22 -related Ritscher-Schinzel syndromes. *Eur. J. Med. Genet.* **65**, 1–7 (2022).
129. C. E. Gjerulfsen, R. S. Møller, C. D. Fenger, T. B. Hammer, A. Bayat, Expansion of the CCDC22 associated ritscher-schinzel/3C syndrome and review of the literature: Should the minimal diagnostic criteria be revised? *Eur. J. Med. Genet.* **64** (2021), doi:10.1016/j.ejmg.2021.104246.
130. C. A. Phillips-Krawczak, A. Singla, P. Starokadomskyy, Z. Deng, D. G. Osborne, H. Li, C. J. Dick, T. S. Gomez, M. Koenecke, J. S. Zhang, H. Dai, L. F. Sifuentes-Dominguez, L. N. Geng, S. H. Kaufmann, M. Y. Hein, M. Wallis, J. McGaughran, J. Gecz, B. Van De Sluis, D. D. Billadeau, E. Burstein, COMMD1 is linked to the WASH complex and regulates endosomal trafficking of the copper transporter ATP7A. *Mol. Biol. Cell*. **26**, 91–103 (2015).
131. P. Bartuzi, D. D. Billadeau, R. Favier, S. Rong, D. Dekker, A. Fedoseienko, H. Fieten, M. Wijers, J. H. Levels, N. Huijkman, N. Kloosterhuis, H. Van Der Molen, G. Brufau, A. K. Groen, A. M. Elliott, J. A. Kuivenhoven, B. Plecko, G. Grangl, J. McGaughran, J. D. Horton, E. Burstein, M. H. Hofker, B. Van De Sluis, CCC- and WASH-mediated endosomal sorting of LDLR is required for normal clearance of circulating LDL. *Nat. Commun.* **7**, 1–11 (2016).
132. D. C. Rubinsztein, The roles of intracellular protein-degradation pathways in neurodegeneration. *Nature*. **443**, 780–786 (2006).
133. F. J. McDonald, Explosion in the complexity of membrane protein recycling. *Am. J. Physiol. - Cell Physiol.* **320**, C483–C494 (2021).
134. L. Muzio, R. Sirtori, D. Gornati, S. Eleuteri, A. Fossaghi, D. Brancaccio, L. Manzoni, L. Ottoboni, L. De Feo, A. Quattrini, E. Mastrangelo, L. Sorrentino, E. Scalone, G. Comi, L. Marinelli, N. Riva, M. Milani, P. Seneci, G. Martino, Retromer stabilization results in neuroprotection in a model of Amyotrophic Lateral Sclerosis. *Nat. Commun.* **11**, 1–17 (2020).
135. S. A. Small, K. Kent, A. Pierce, C. Leung, M. S. Kang, H. Okada, L. Honig, J. P. Vonsattel, T. W. Kim, Model-guided microarray implicates the retromer complex in Alzheimer's disease. *Ann. Neurol.* **58**, 909–919 (2005).
136. E. Rogaeva, Y. Meng, J. H. Lee, Y. Gu, T. Kawarai, F. Zou, T. Katayama, C. T. Baldwin, R. Cheng, H. Hasegawa, F. Chen, N. Shibata, K. L. Lunetta, R. Pardossi-Piquard, C. Bohm, Y. Wakutani, L. A. Cupples, K. T. Cuenco, R. C. Green, L. Pinessi, I. Rainero, S. Sorbi, A. Bruni, R. Duara, R. P. Friedland, R. Inzelberg, W. Hampe, H. Bujo, Y. Q. Song, O. M. Andersen, T. E. Willnow, N. Graff-Radford, R. C. Petersen, D. Dickson, S. D. Der, P. E. Fraser, G. Schmitt-Ulms, S. Younkin, R. Mayeux, L. A. Farrer, P. St. George-Hyslop, The neuronal sortilin-related receptor SORL1 is genetically associated with Alzheimer disease. *Nat. Genet.* **39**, 168–177 (2007).
137. R. F. Lane, S. M. Raines, J. W. Steele, M. E. Ehrlich, J. A. Lah, S. A. Small, R. E. Tanzi, A. D. Attie, S. Gandy, Diabetes-associated SorCS1 regulates Alzheimer's amyloid-β metabolism: Evidence for involvement of SorL1 and the retromer complex. *J. Neurosci.* **30**, 13110–13115 (2010).
138. F. L. Tang, W. Liu, J. X. Hu, J. R. Erion, J. Ye, L. Mei, W. C. Xiong, VPS35 Deficiency or Mutation Causes Dopaminergic Neuronal Loss by Impairing Mitochondrial Fusion and Function. *Cell Rep.* **12**, 1631–1643 (2015).
139. L. R. Yohe, K. T. J. Davies, N. B. Simmons, K. E. Sears, E. R. Dumont, S. J. Rossiter, L. M. Dávalos, Evaluating the performance of targeted sequence capture, RNA-Seq, and degenerate-primer PCR cloning for sequencing the largest mammalian multigene family. *Mol. Ecol. Resour.* **20**, 140–153 (2020).
140. R. Tacutu, D. Thornton, E. Johnson, A. Budovsky, Di. Barardo, T. Craig, E. DIana, G. Lehmann, D. Toren, J. Wang, V. E. Fraifeld, J. P. De Magalhães, Human Ageing Genomic Resources: New and updated databases. *Nucleic Acids Res.* **46**, D1083–D1090 (2018).
141. S. Chen, Y. Zhou, Y. Chen, J. Gu, Fastp: An ultra-fast all-in-one FASTQ preprocessor. *Bioinformatics*. **34**, i884–i890 (2018).
142. N. L. Bray, H. Pimentel, P. Melsted, L. Pachter, Near-optimal probabilistic RNA-seq

quantification. *Nat. Biotechnol.* **34**, 525–527 (2016).
143. D. M. Emms, S. Kelly, OrthoFinder: Phylogenetic orthology inference for comparative genomics. *Genome Biol.* **20**, 1–14 (2019).
144. C. W. Dunn, F. Zapata, C. Munro, S. Siebert, A. Hejnol, Pairwise comparisons across species are problematic when analyzing functional genomic data. *Proc. Natl. Acad. Sci. U. S. A.* **115**, E409–E417 (2018).
145. S. Álvarez-Carretero, A. U. Tamuri, M. Battini, F. F. Nascimento, E. Carlisle, R. J. Asher, Z. Yang, P. C. J. Donoghue, M. dos Reis, A species-level timeline of mammal evolution integrating phylogenomic data. *Nature*. **602**, 263–267 (2022).
146. D. W. Huang, B. T. Sherman, R. A. Lempicki, Systematic and integrative analysis of large gene lists using DAVID bioinformatics resources. *Nat. Protoc.* **4**, 44–57 (2009).
147. L. G. Mengjun, TCseq: Time course sequencing data analysis. R package version 1.8.0., 1–8 (2019).
148. M. I. Love, W. Huber, S. Anders, Moderated estimation of fold change and dispersion for RNA-seq data with DESeq2. *Genome Biol.* **15**, 1–21 (2014).
149. Y. Benjamini, Y. Hochberg, Controlling the False Discovery Rate□: A Practical and Powerful Approach to Multiple Testing. *J. R. Stat. Soc.* **57**, 289–300 (1995).

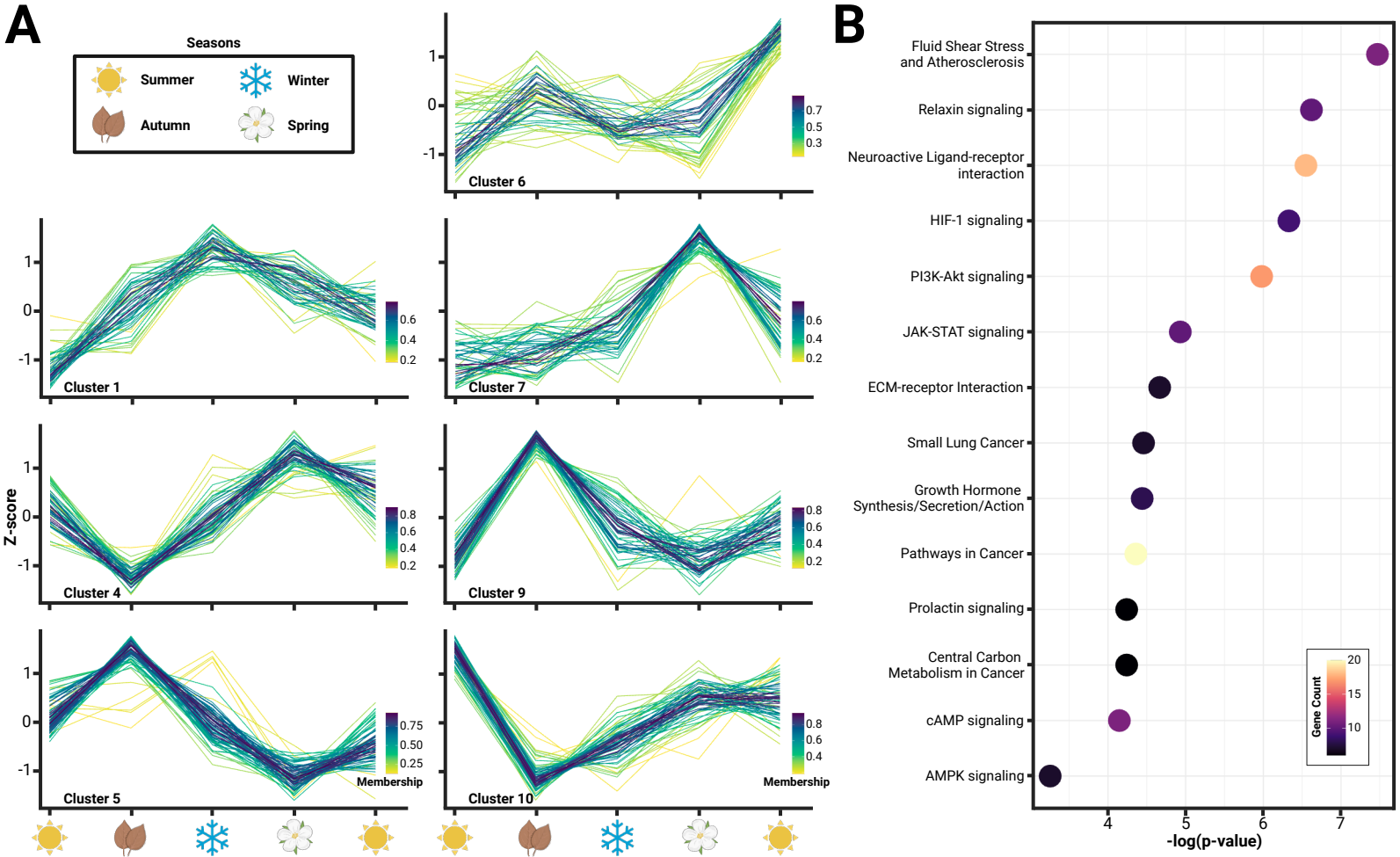
A
Seasons
Summer
Winter
Autumn
Spring
Cluster 1
Cluster 4
Cluster 5
Cluster 6
Cluster 7
Cluster 9
Cluster 10
Z-score
Membership
B
Fluid Shear Stress and Atherosclerosis
Relaxin signaling
Neuroactive Ligand-receptor interaction
HIF-1 signaling
PI3K-Akt signaling
JAK-STAT signaling
ECM-receptor Interaction
Small Lung Cancer
Growth Hormone Synthesis/Secretion/Action
Pathways in Cancer
Prolactin signaling
Central Carbon Metabolism in Cancer
cAMP signaling
AMPK signaling
Gene Count
-log(p-value)

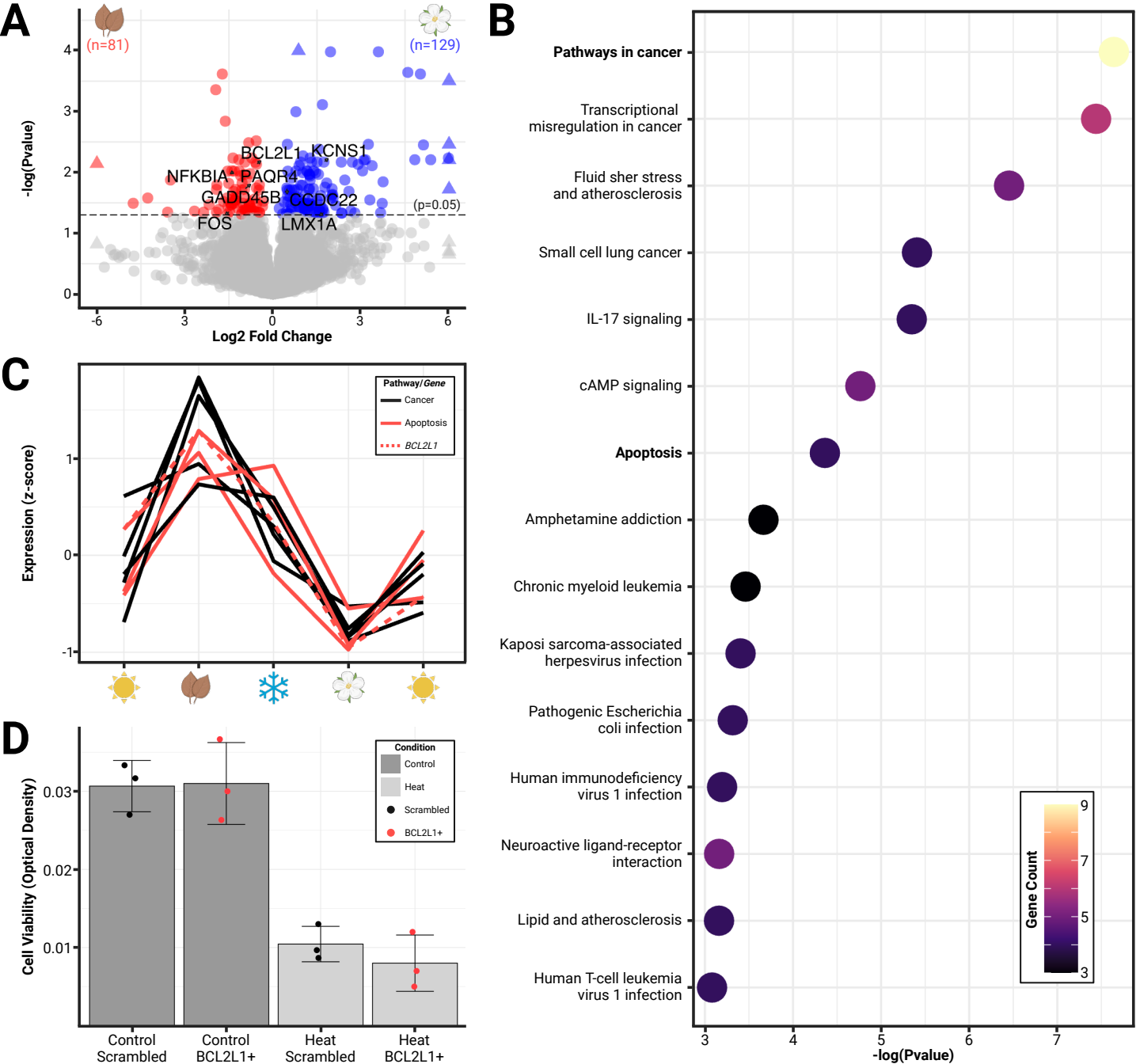
A
(n=81)
(n=129)
-log(Pvalue)
Log2 Fold Change
BCL2L1
KCNS1
NFKBIA
PAQR4
GADD45B
CCDC22
FOS
LMX1A
(p=0.05)
B
Pathways in cancer
Transcriptional misregulation in cancer
Fluid sher stress and atherosclerosis
Small cell lung cancer
IL-17 signaling
cAMP signaling
Apoptosis
Amphetamine addiction
Chronic myeloid leukemia
Kaposi sarcoma-associated herpesvirus infection
Pathogenic Escherichia coli infection
Human immunodeficiency virus 1 infection
Neuroactive ligand-receptor interaction
Lipid and atherosclerosis
Human T-cell leukemia virus 1 infection
-log(Pvalue)
Gene Count
C
Expression (z-score)
Pathway/Gene
Cancer
Apoptosis
BCL2L1
D
Cell Viability (Optical Density)
Condition
Control
Heat
Scrambled
BCL2L1+
Control Scrambled
Control BCL2L1+
Heat Scrambled
Heat BCL2L1+

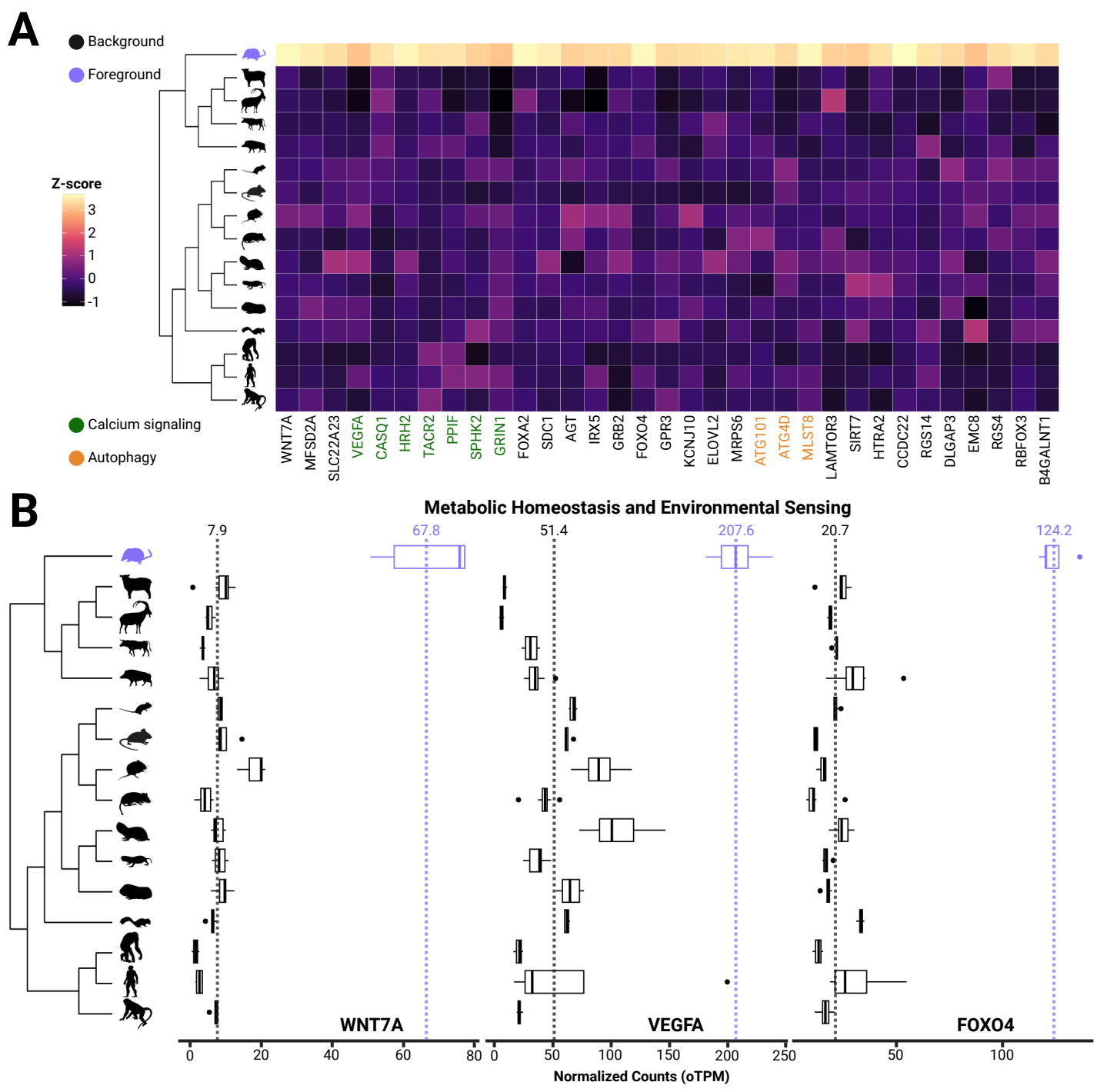
A
Background
Foreground
Z-score
3
2
1
0
-1
Calcium signaling
Autophagy
WNT7A
MFSD2A
SLC22A23
VEGFA
CASQ1
HRH2
TACR2
PPIF
SPHK2
GRIN1
FOXA2
SDC1
AGT
IRX5
GRB2
FOXO4
GPR3
KCNJ10
ELOVL2
MRPS6
ATG101
ATG4D
MLST8
LAMTOR3
SIRT7
HTRA2
CCDC22
RGS14
DLGAP3
EMC8
RGS4
RBFOX3
B4GALNT1
B
Metabolic Homeostasis and Environmental Sensing
7.9
67.8
51.4
207.6
20.7
124.2
WNT7A
VEGFA
FOXO4
0
20
40
60
80
0
50
100
150
200
250
50
100
Normalized Counts (oTPM)

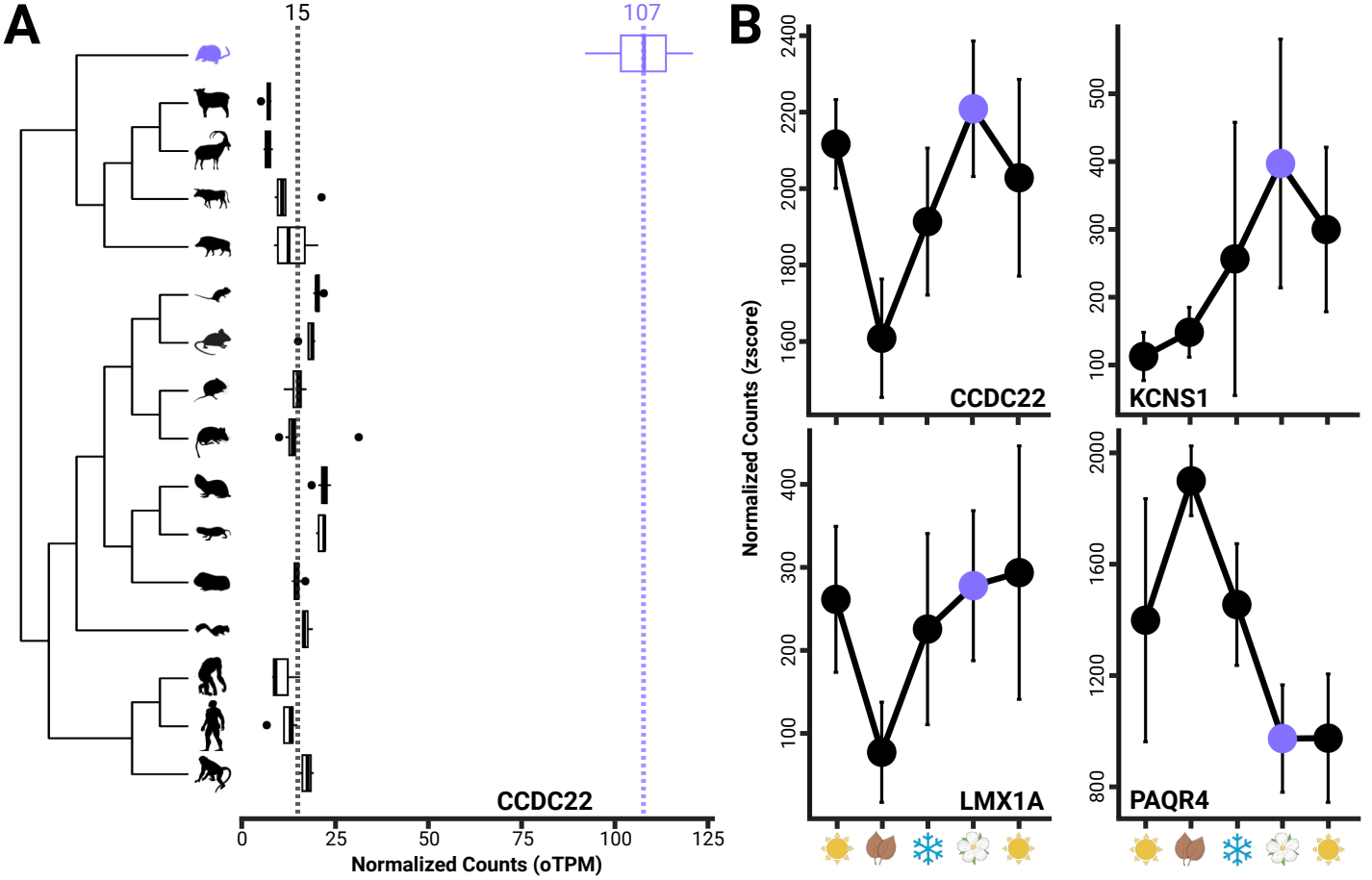
A
15
107
CCDC22
0
25
50
75
100
125
Normalized Counts (oTPM)
B
Normalized Counts (zscore)
CCDC22
KCNS1
LMX1A
PAQR4